



Treball Final de Grau

Study of a Biogas Combustion Chamber Using a Computational Fluid Dynamics Software (ANSYS®)

Estudi d'una Càmera de Combustió de Biogàs Utilitzant un Software de Dinàmica de Fluids Computacional (ANSYS®)

Salvador Vilas Bonafoux

June, 2016



**UNIVERSITAT DE
BARCELONA**

Aquesta obra esta subjecta a la llicència de:
Reconeixement–NoComercial–SenseObraDerivada



<http://creativecommons.org/licenses/by-nc-nd/3.0/es/>

A true master is an eternal student

Anonymous

En primer lloc, agrair als meus pares tot l'esforç i confiança que han dipositat en mi, ja que sense ells res d'això hauria estat possible. També els ànims i el suport que m'han donat durant aquests quatre anys, que m'han ajudat a seguir endavant en els moments més difícils.

A continuació, donar les gràcies als meus tutors, Jordi Bonet i Alexandra Bonet, per tot el temps i paciència que han tingut amb mi i amb la resta dels meus companys per ajudar-nos i estar al nostre costat constantment. També aprofito per donar les gràcies al que ha estat el meu tutor durant el grau, Carles Fité, i a la resta del professorat, per tot el que m'han ensenyat i per haver-me ajudat a créixer com a persona i com a professional.

Finalment, no puc oblidar els meus companys de classe, companys de pis i amics en general que han fet que la meva estància a Barcelona hagi sigut una experiència única i inoblidable per mi.

REPORT

CONTENTS

1. SUMMARY	3
2. RESUM	5
3. INTRODUCTION	7
3.1. Other biogas simulations	8
3.2. Adding water to combustion systems	10
3.3. Biogas upgrading	12
4. OBJECTIVES	14
5. MATERIALS AND METHODS: USING ANSYS® FLUENT	15
5.1. Performing a simulation	15
5.1.1. Geometry design	15
5.1.2 Mesh generation	17
5.1.3 Simulation setup	18
6. SENSITIVITY ANALYSIS	22
7. RESULTS AND INTERPRETATION	31
7.1. Temperature profiles	35
7.2. NO _x ppm profiles	44
8. CONCLUSIONS	53
9. REFERENCES AND NOTES	55
10. ACRONYMS	57
APPENDICES	59
APPENDIX 1: THERMAL NO_x RATE PROFILES	61
APPENDIX 2: PROMPT NO_x RATE PROFILES	69

1. SUMMARY

This final degree project is a study of the consequences of using biogas or adding water to a combustion chamber. A sensitivity analysis with the computational fluid dynamics software ANSYS® Fluent has been performed to quantify these effects, focusing on the polluting impacts and more specifically on the NO_x formation.

First of all, an abstract of the most relevant studies that show up when looking for some of the ideas related to this study will be exposed. Then, some explanations about how does ANSYS® Fluent work will be given, in order to make this study easy to understand. Finally, the results obtained during this project will be showed, accompanied by an interpretation and an analysis of them.

Keywords: combustion, biogas, ANSYS, NO_x

2. RESUM

Aquest treball final de grau és un estudi sobre les conseqüències d'utilitzar biogàs o afegir aigua a una càmera de combustió. Per a quantificar aquests efectes, s'ha realitzat una anàlisi de sensibilitat amb el software de dinàmica de fluids computacional ANSYS® Fluent, fent èmfasi en els impactes contaminats i més específicament en la formació de NO_x .

En primer lloc, es mostrarà un abstracte dels estudis més rellevants que apareixen quan es busquen idees relacionades amb aquest estudi. A continuació, es donaran algunes explicacions sobre com funciona ANSYS® Fluent per a que el treball sigui fàcil d'entendre. Finalment, es presentaran els resultats obtinguts durant aquest projecte, acompanyats d'una interpretació i una anàlisi dels mateixos.

Paraules clau: combustió, biogàs, ANSYS, NO_x

3. INTRODUCTION

The high and growing demand for energy in today's world has been met about 80% with a fossil fuel supply. Fossil fuel reserve is questionable and the use of fossil fuel resulted in the increase of unwanted pollutants emission. This condition requires urgent development of improved pollutants process and new sources of energy other than fossil fuel. Biogas is one of the options since it is renewable and carbon dioxide produced in the combustion process will be used back by the biomass that grown to produce biogas.

Biogas has a wide range of applications. It can be used for electricity production on sewage works, in a CHP (Combined Heat and Power) gas engine, where the waste heat from the engine is conveniently used for process heating, space heating, water heating, etc. If compressed, it can replace compressed natural gas for use in vehicles, where it can fuel an internal combustion engine or fuel cells. Since it is more than likely that biogas will play an important role as an energy source in the near future, it is a very attractive field of study for many reasons.

Firstly, since it is a relatively new source of energy, the efficiency of these combustion systems must be maximized in order to obtain the higher possible profit from them. Moreover, not only the concern about the efficiency motivates the studies about its combustion, but also these processes must be environmentally friendly. One of the most limiting aspects for the optimization of biogas combustion systems is the pollution associated to them. For example, CO₂ and some VOC's (Volatile Organic Compounds) are related with global warming, SO_x produces acid rain, CO bonds with hemoglobin (disabling it) and finally NO_x causes pollution in big cities and is currently an important matter of concern.

On the other hand, the power of computing technologies has experienced a very important increase in the last years, which allows to perform simulations that can be useful for a first approach and save time and resources in expensive experiments.

The effects that water addition has in the NO_x formation will be studied, as there is an important concern about the production of this pollutant and possible measures to tackle this problem are needed.

3.1. OTHER BIOGAS SIMULATIONS

Some interesting examples can be found when looking for studies of biogas combustors using CFD. It is more than likely that *Noor et al (2013)* is the most similar study to this project. Although the geometry used in that study is different from the one that is analyzed in this project, the main ideas are quite similar: it performs a sensitivity analysis using ANSYS® Fluent to predict the NO_x formation of a bluff-body MILD (Moderate and Intense Low oxygen Dilution) burner. This burner has an important feature: part of the exhaust gases are recirculated and introduced again to the furnace. This device is observed in Figure 1.



Figure 1: Bluff-body MILD combustor. (*Noor et al, 2013*)

Noor et al (2013) explains step by step the CFD simulation for the non-premixed MILD combustion furnace with biogas as fuel. Although the image above is in 3D, the calculation is run in 2D, like in this project. However, no precision or accuracy is lost, due to the fact that both this furnace and the one used in this project have a complete symmetry that allows to assume no variation in the radial coordinate. This technique is widely used, as it reduces the computational time and cost and does not affect the results.

The above explanation is illustrated in Figure 2, where all the needed information has been calculated only in a symmetry plane.



Figure 2: Velocity profiles for the MILD combustor. (Noor et al, 2013)

Another very interesting study, although not related to combustion, is given by *Latha et al (2009)*. In this paper, the authors perform different CFD simulations of an anaerobic digester at the same time that they carry out the real experiments in a laboratory scale reactor. This is very useful, because one can check if the results obtained using the software program are similar or not to the obtained in a real experiment.

The main idea behind this paper is to use CFD simulations to predict the behavior that the system will have in reality without having to perform a real experiment. In fact, a viscosity and mixing study is carried out, and CFD simulations' purpose is to give an idea about the time that will take to reach the steady state and when and where will be dead zones due to high viscosity.

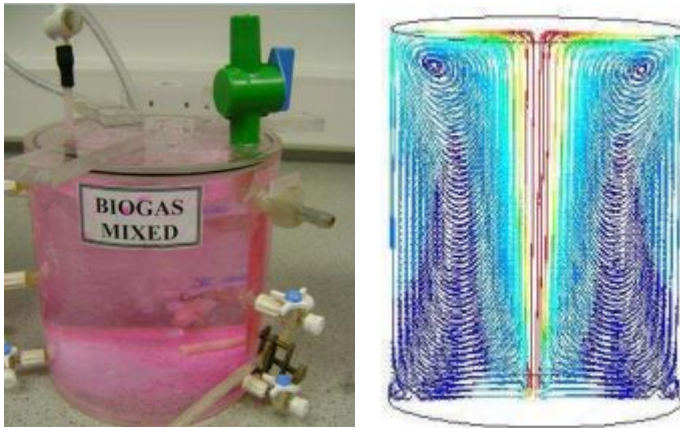


Figure 3: Real experiment (left) and CFD simulation (right). (Latha et al, 2009)

3.2. ADDING WATER TO COMBUSTION SYSTEMS

Although they might seem innovative, water-injection engines began to be used several decades ago. At the beginning, water-injection's purpose was to work as an intercooler: taking advantage of water's high heat of vaporization, heat is transferred from the hot cylinder air into the water, evaporating it and cooling the intake charge. Therefore, the intake charge is denser and thus the volumetric efficiency is higher. Furthermore, it also prevents that some hot points produce premature ignition, and in jet engines increases the thrust of the engine, which is very useful at low speeds and takeoff, while also cools the turbines.

Water-injection engines are mainly used in aircrafts and in automobiles. For example, the 1957 Boeing KC-135 used water during takeoff to have an extra power. This is known as a wet takeoff, and seen in Figure 4.



Figure 4: Boeing KC-135 performing a wet takeoff. (USAF, 2013)

In automobiles, a very recent example can be mentioned. The 2015 BMW M4 GTS features a water-injection engine, which is used both to increase the engine's power and to reduce pollutant emissions. Keeping in mind that it is the fastest BMW road car ever and that its price is above 150 000 €, and furthermore being the Moto GP official safety car, it is more than likely that the tendency of adding water to engines will increase its popularity in the near future. The system that this car features is shown in Figure 5.



Figure 5: BMW M4 GTS water-injection system. (BMW, 2015)

However, regarding this study, the most interesting advantage of adding water to a combustion chamber is the reduction of NO_x formation. This reduction is due to two reasons: first of all, the peak temperature of the system decreases when water is added, which makes that the thermal NO_x formation is also decreased, as will be explained in more detail in the following section. Additionally, the presence of water influences directly the reaction mechanism. According to *Chybowski et al (2015)*, the water supplied into the combustion chamber reduces the concentration of atomic oxygen and promotes the formation of hydrogenated species such as HCN or HNCO, which cannot convert directly to NO. To explain the behavior previously described, Figures 6 and 7 are added.

water washing is the most used method, the composition of a biogas upgraded with this method will be used in this study. *Rasi (2009)* published a study where biomethane composition was analyzed, to see the differences of using different upgrading processes while using the same raw biogas. In the case of water washing, *Rasi (2009)* saw that depending on the water flow rate and gas flow rate used in the process, the obtained biomethane had different compositions. In this study, the composition chosen is a mean of the four compositions given in the previous mentioned paper, which is going to be detailed in the following section.

The industrial process to obtain biomethane by using the water washing cleaning method is shown in Figure 8.

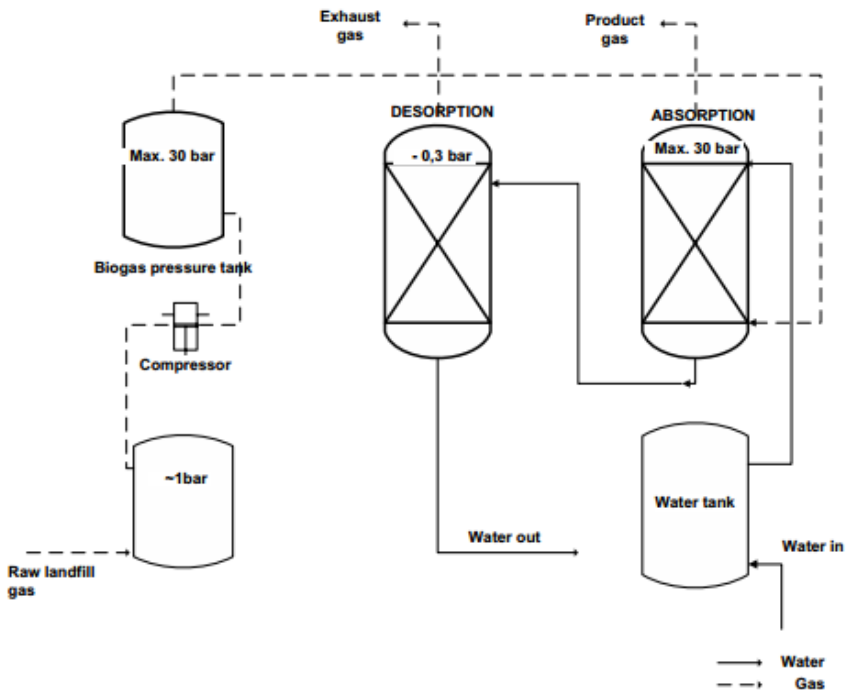


Figure 8: Simplified diagram of the counter-current water wash upgrading process. (*Rasi, 2009*)

4. OBJECTIVES

The aim of the project is performing a CFD (Computational Fluid Dynamics) analysis using the simulation tool ANSYS® allowing to study many different aspects about the system in detail and to reduce the time spent in research. Taking advantage of this tool, this study has the following objectives:

- To study the water addition effect in a combustion chamber that is burning biogas by quantifying the NO_x production when different quantities of water are added, either to the fuel or to the air.
- To perform the same study keeping all the parameters constant except the fuel, which is industrial methane.
- To compare both analysis to see which of the fuels has the most negative environmental impact, as it is wanted to know if biogas could be a better choice than methane in terms of pollution.

5. MATERIALS AND METHODS: USING ANSYS® FLUENT

CFD is one of the ways to virtually design and run a simulation experiment without the need to physically build the model. The cost of model building and repeat the process until the desired result is quite large. This process can be done by CFD modelling using commercial software and is much cheaper compared to building the physical unit.

The precision and accuracy that are going to be obtained performing a CFD analysis very much depend on selecting the appropriate models. In the following subsections, the chosen models are explained, and reasons why they are used are given.

5.1. PERFORMING A SIMULATION

As commented before, ANSYS® provides access to multiple modules that allow to simulate a huge number of scenarios focusing on a lot of different engineering areas. Fluent is one of these modules, and its characteristics and models are suitable for the combustor that is going to be studied in this project.

To make this study more understandable, a brief explanation of how does the software program work and what does the user need to do to perform a simulation is provided. Every step that has to be followed to successfully perform a simulation is explained, focusing on the models and on the NO_x formation setup, which are the most critical steps of the simulation.

The previous mentioned steps that have to be completed in order to perform a calculation are the following:

- Geometry design
- Mesh generation
- Models set up
- Establishment of the calculation parameters
- Results review and visualization

5.1.1. Geometry design

When a new simulation is started, the first thing to do is to set the geometry that is wanted to be analyzed. To do it, ANSYS® offers different tools that allow to draw any kind of geometry.

Moreover, a geometry from another drawing software such as AutoCAD, Solidworks or Unigraphic can be imported to ANSYS®, which is a very useful feature.

The combustion chamber used in this project represents the geometry of a 300kW swirl-stabilized burner. As mentioned before, the system has a high level of symmetry which allows to reduce the calculation domain to a 2D problem, which drastically reduces the computational time to calculate the solution. The calculation domain is shown in Figure 9.

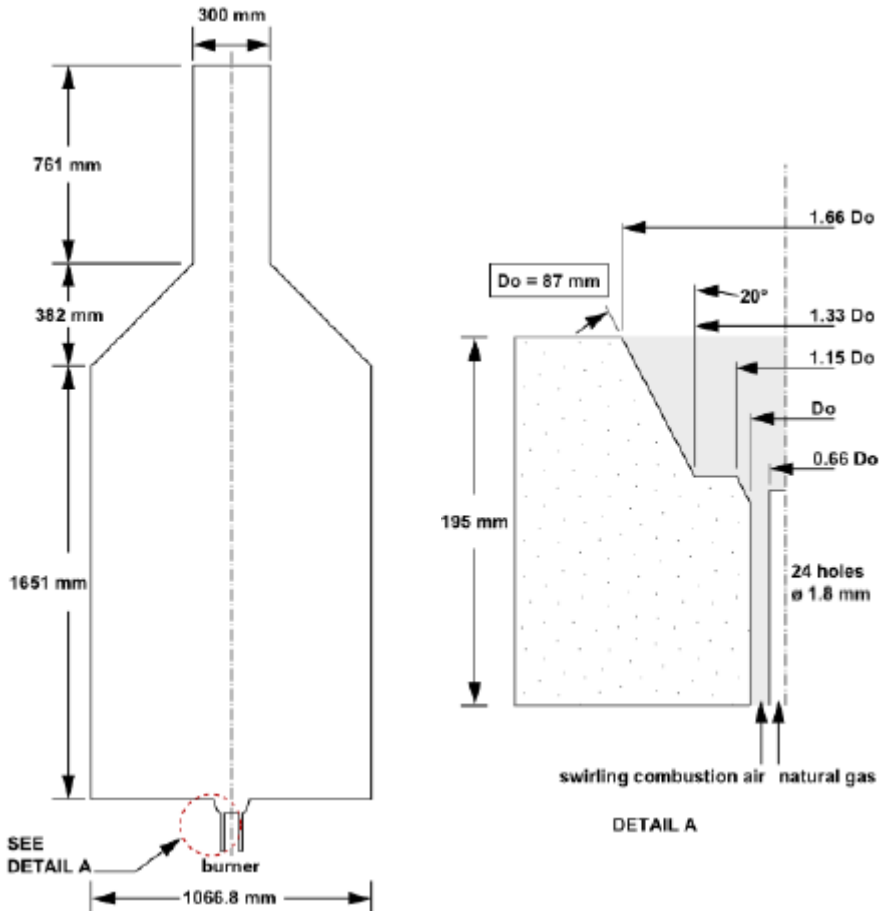


Figure 9: Calculation domain of the combustion chamber. (ANSYS®, 2015)

5.1.2. Mesh generation

Once the geometry has been drawn, the system must be discretized in order to solve the mathematical model. If the system wanted to be solved without discretizing it, microscopic balances should be solved, which are differential equations. By discretizing the system, finite elements are created, and its size is such small that those differential equations from the microscopic balances can be transformed to algebraic equations, which require less effort to be calculated. This is called the finite elements method.

Obviously, the solution is not completely exact because the equations' transformation is just an approximation. This approximation will be better as finite elements size is reduced. However, as smaller is the finite elements size, bigger is the number of points that have to be calculated. This is why a mesh cannot be too refined, otherwise the computational time to perform the simulation would be too high. To minimize the error, a very common strategy is to create inflation zones. Basically, it consists of mesh refining only in the zones where a lot of changes are going to happen, such as inlets, intense chemical reactions, etc. By doing this, the accuracy is increased in the most important zones while the computational time is still reasonable.

In the combustion chamber used in this study, the zones that need an inflation are the fuel inlet and the symmetry axis, because is where the major part of the combustion will take place. The mesh and the inflation zones are showed in Figures 10 and 11.

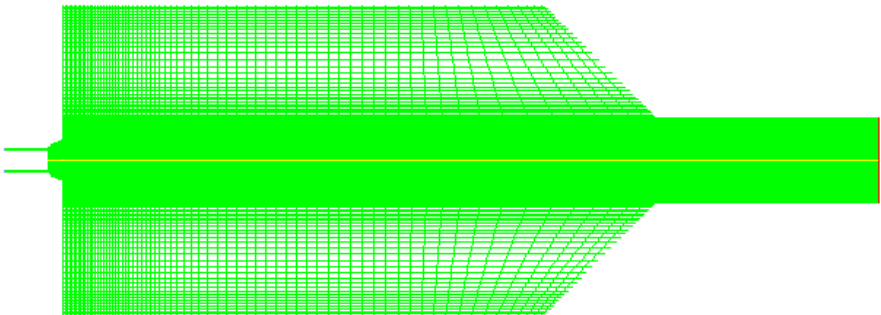


Figure 10: Final mesh. The inflation zone around the symmetry axis can be appreciated.

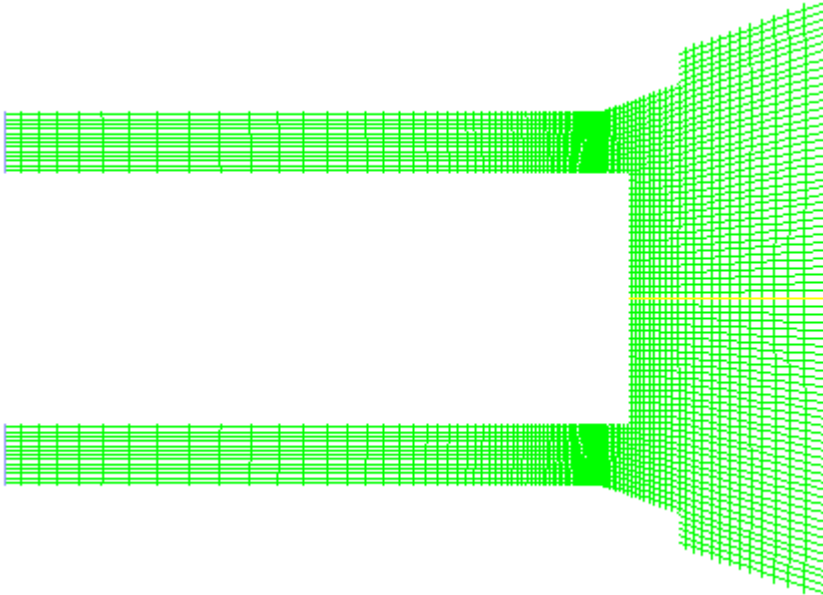


Figure 11: Zoom-in at the inflation zone of the fuel inlet.

5.1.3. Simulation setup

In this step is where Fluent module is properly used. The two previous steps are general for any ANSYS® simulation, and once completed, the appropriate module is chosen. This is probably the most important part of the simulation, because it is about choosing the correct models, and is crucial to obtain a reliable solution. In this part, the models are set, the boundary conditions are defined and the solution methods and controls are established.

In the model definition section, one must take into account the mathematical model that governs the process to analyze. In Fluent case, the mathematical model is composed of fluid flow equations, which are series of balances and fluid properties, including the overall mass balance (also known as the continuity equation), the momentum balance, the energy balance (which is decomposed in different equations) and partial mass balances. These equations are:

Continuity

$$\frac{\delta \rho U}{\delta t} + \nabla \cdot \rho U = 0$$

Momentum

$$\frac{\delta \rho U}{\delta t} + (\nabla \cdot \rho U U) = -\nabla p + \nabla \cdot \tau + \rho g$$

Enthalpy

$$\frac{\delta \rho h}{\delta t} + \nabla \cdot \rho U = \nabla \cdot \lambda_e \nabla T - \nabla \cdot q_r + \nabla \cdot \sum_l \rho h_l(T) D_e \nabla m_l$$

Temperature

$$\rho C_p \frac{DT}{Dt} = \nabla \cdot \lambda_e \nabla T - \nabla \cdot \sum_l \rho h_l(T) D_e \nabla m_l - \rho \sum_l \frac{Dm_l}{Dt} h_l(T)$$

Species mass fraction

$$\frac{\delta \rho m_l}{\delta t} + \nabla \cdot \rho U m_l = \nabla \cdot D_e \rho \nabla m_l - R_l$$

To solve the problem, Fluent discretizes these governing equations for each point generated in the meshing section. But apart from the previous mentioned equations, Fluent offers different additional models that can be activated depending on the system that is going to be studied. In this case, four additional models must be activated in order to perform the simulation as accurately as possible.

First of all, viscous model must be activated because there is a fluid flowing through the system. Due to high velocity inlet (around 160 m/s for the fuel) and swirl's presence, turbulent flow is expected, and therefore an appropriate model is needed to be chosen. The most accepted and used method to perform calculations where turbulent flow is present is the k-epsilon model, which consists of two equations, one for the turbulent kinetic energy (k) and one for the turbulent dissipation rate (epsilon). These equations are:

Turbulent kinetic energy (k)

$$\frac{\delta(\rho k)}{\delta t} + \frac{\delta(\rho k u_i)}{\delta x_i} = \frac{\delta}{\delta x_j} \left[\left(\mu + \frac{\mu_t}{\sigma_k} \right) \frac{\delta k}{\delta x_j} \right] + P_k + P_b + \rho \epsilon - Y_M + S_k$$

Turbulent dissipation rate (epsilon)

$$\frac{\delta(\rho \epsilon)}{\delta t} + \frac{\delta(\rho \epsilon u_i)}{\delta x_i} = \frac{\delta}{\delta x_j} \left[\left(\mu + \frac{\mu_t}{\sigma_\epsilon} \right) \frac{\delta \epsilon}{\delta x_j} \right] + C_{1\epsilon} \frac{\epsilon}{k} (P_k + C_{3\epsilon} P_b) - \rho C_{2\epsilon} \frac{\epsilon^2}{k} + S_\epsilon$$

Then, also the radiation model has to be activated because in the combustion chamber, temperatures above 2200K are achieved. The P-1 radiation model will be applied, which is the simplest particular case of the P-N model. The radiation flux term in the energy balance is provided by the following equation:

$$-\nabla \cdot q_r = aG - 4an^2\sigma T^4$$

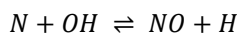
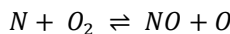
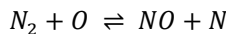
where a is the absorption coefficient, n is the refractive index of the medium, σ is the Stefan-Boltzmann constant and G is the incident radiation.

Afterwards, the appropriate species model is chosen. In this case, the non-premixed model is activated, because it is used when the oxidizer and the fuel enter the combustion chamber in different streams. This method reduces the thermochemistry of the problem to a single parameter, assuming some simplifications. This parameter is called the mixture fraction, and it establishes a relation between the burned and the unburned fuel stream elements. Therefore, all the species parameters required for the transport equations are defined in terms of the mixture fraction, which allows to simplify the difficulties of determining them using non-linear equations. The mixture fraction has the following expression:

$$f = \frac{Z_i - Z_{i,OX}}{Z_{i,fuel} - Z_{i,OX}}$$

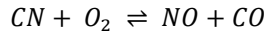
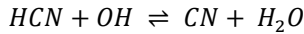
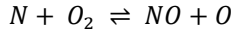
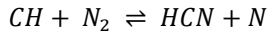
where Z_i is the elemental mass fraction of the element i and the subscripts *OX* and *fuel* denote the value at the oxidizer stream inlet and at the fuel stream inlet respectively. As can be seen, the value of the mixture fraction will be always between 0 and 1, which gives an idea about how burned is a certain element in a very simple way.

Finally, regarding the fact that one of the most important objectives of this study is to determine the pollutant formation, a model to calculate NO_x formation is set. The three primary pathways of NO_x formation in combustion processes are thermal NO_x , fuel NO_x and prompt NO_x . First of all, thermal NO_x refers to NO_x formed through high temperature (usually above 1600 °C) oxidation of the diatomic nitrogen found in combustion air, and is recognized as the most relevant source in combustion. The main reactions producing thermal NO_x are described in the extended Zeldovich mechanism:



These reactions are highly temperature dependent, because the N_2 triple bond requires to be broken. In fact, it is estimated that the NO_x production rate doubles for every 90 K temperature increase when system temperature is above 2200 K.

Then, prompt NO_x is attributed to the reaction of atmospheric nitrogen, N_2 , with radicals derived from fuel. Although it is usually the minor contribution in NO_x formation, it becomes relevant in low temperature combustions of oxygenated fuels. However, as NO_x emissions are nowadays reduced to very low levels, even a small contribution has to be taken into account. It occurs in the earliest stage of combustion, and its mechanism is the following:



Fuel NO_x is not calculated in this experiment, because it is associated with nitrogenous hydrocarbons, which are not present in any of the two studied fuels.

6. SENSITIVITY ANALYSIS

Now that all the models are described and properly activated, the simulation can be carried out. As commented before, the effect of water addition into the combustor is studied. This is done by performing different simulations maintaining all the variables constant and only changing the amount of water added in the system. This is called a parametric analysis.

As mentioned in the Objectives section, one of the objectives of this project is to compare the pollutant emission of an upgraded biogas (also called biomethane) and an industrial methane. Biomethane composition has been extracted from *Rasi (2009)* while methane composition was obtained from Union Gas Ltd Company, a Canadian natural gas storage, transmission and distribution company. These compositions are shown in Tables 1 and 2.

Table 1. Biomethane composition. (*Rasi, 2009*)

Species	Mole fraction
CH ₄	$9.00 \cdot 10^{-1}$
N ₂	$6.00 \cdot 10^{-2}$
CO ₂	$3.99 \cdot 10^{-2}$
C ₂ H ₆	$3.20 \cdot 10^{-5}$
C ₃ H ₈	$3.00 \cdot 10^{-5}$
C ₄ H ₁₀	$1.76 \cdot 10^{-5}$
C ₆ H ₆	$2.00 \cdot 10^{-5}$
H ₂ S	$2.50 \cdot 10^{-7}$
CH ₃ Cl	$1.50 \cdot 10^{-7}$

Table 2. Methane composition. (*Union Gas Ltd*)

Species	Mole fraction
CH ₄	$9.50 \cdot 10^{-1}$
N ₂	$1.00 \cdot 10^{-2}$
CO ₂	$5.00 \cdot 10^{-3}$
C ₂ H ₆	$3.19 \cdot 10^{-2}$
C ₃ H ₈	$2.00 \cdot 10^{-3}$
C ₄ H ₁₀	$6.00 \cdot 10^{-4}$
C ₅ H ₁₂	$2.00 \cdot 10^{-4}$
C ₆ H ₁₄	$1.00 \cdot 10^{-4}$
O ₂	$2.00 \cdot 10^{-4}$

Water is added both in air and fuel inlets, because not only the amount of water affects the system but also the contact model has to be taken into account. To make the study reliable, when water is added, the flow rate of the inlet stream needs to be changed in order to keep the fuel/air ratio constant in all the experiments. Otherwise, adding water would mean adding less fuel or air, which would conduct to false results. To do it, the inlet velocity has been changed in proportion to the added water, so that the air or fuel mass flow rate maintains constant. The amount of water added is referred to the mass fraction of CH₄ present in the fuel, and varies from 0% to 25% in 5% increments. The velocities used are shown in Tables 3 and 4.

Table 3. Biomethane velocity inlets.

Inlet with water	Water percentage	Velocity [m/s]
Fuel	5	163.60
	10	169.94
	15	176.29
	20	182.64
	25	188.98
Air	5	32.05
	10	32.09
	15	32.14
	20	32.18
	25	32.23

Table 4. Industrial methane velocity inlets.

Inlet with water	Water percentage	Velocity [m/s]
Fuel	5	164.36
	10	171.47
	15	178.58
	20	185.69
	25	192.80
Air	5	32.05
	10	32.09
	15	32.14
	20	32.18
	25	32.23

In both cases, the velocity inlet for fuel and water was 157.25 m/s and 32 m/s respectively in the dry case (0% water). Finally, compositions used in each simulation are shown in Tables 5 and 6, one for each fuel.

Table 5. Biomethane compositions for each water percentage (mole fraction).

Species	Water percentage				
	5	10	15	20	25
H ₂ O	3.85E-02	7.41E-02	1.07E-01	1.38E-01	1.67E-01
CH ₄	8.65E-01	8.33E-01	8.04E-01	7.76E-01	7.50E-01
N ₂	5.77E-02	5.56E-02	5.36E-02	5.17E-02	5.00E-02
CO ₂	3.84E-02	3.69E-02	3.56E-02	3.44E-02	3.33E-02
C ₂ H ₆	3.08E-05	2.96E-05	2.86E-05	2.76E-05	2.67E-05
C ₃ H ₈	2.88E-05	2.78E-05	2.68E-05	2.59E-05	2.50E-05
C ₄ H ₁₀	1.69E-05	1.63E-05	1.57E-05	1.52E-05	1.47E-05
C ₆ H ₆	1.92E-05	1.85E-05	1.79E-05	1.72E-05	1.67E-05
H ₂ S	2.40E-07	2.31E-07	2.23E-07	2.16E-07	2.08E-07
CH ₃ Cl	1.44E-07	1.39E-07	1.34E-07	1.29E-07	1.25E-07

Table 6. Methane compositions for each water percentage (mole fraction).

Species	Water percentage				
	5	10	15	20	25
H₂O	4.05E-02	7.79E-02	1.12E-01	1.44E-01	1.74E-01
CH₄	9.12E-01	8.76E-01	8.43E-01	8.13E-01	7.84E-01
N₂	3.06E-02	2.94E-02	2.83E-02	2.73E-02	2.63E-02
CO₂	1.92E-03	1.84E-03	1.78E-03	1.71E-03	1.65E-03
C₂H₆	5.76E-04	5.53E-04	5.33E-04	5.13E-04	4.95E-04
C₃H₈	1.92E-04	1.84E-04	1.78E-04	1.71E-04	1.65E-04
C₄H₁₀	9.59E-05	9.22E-05	8.88E-05	8.56E-05	8.26E-05
C₅H₁₂	9.59E-03	9.22E-03	8.88E-03	8.56E-03	8.26E-03
C₆H₁₄	4.80E-03	4.61E-03	4.44E-03	4.28E-03	4.13E-03
O₂	1.92E-04	1.84E-04	1.78E-04	1.71E-04	1.65E-04

In the following section, in order to abbreviate, cases with water in fuel will be named WF while cases with water in air will be named WA.

7. RESULTS AND INTERPRETATION

As described before, one of the most important parameters involved in NO_x formation is the temperature of the system, as it has a very important influence on thermal NO_x rate. For this reason, four profiles will be exposed for each simulation: temperature, NO_x ppm, thermal NO_x and prompt NO_x .

First of all, a graphic with the NO_x ppm of each simulation is shown, to give an idea about the order of magnitude that is being obtained and to quickly see the water addition effect. To compute NO_x parts per million, a custom function is introduced. With it, dry ppm are calculated by removing the water mole fraction in the denominator. The formula is:

$$\text{NO}_x \text{ ppm} = \frac{\text{NO}_{mole \text{ fraction}} \cdot 10^6}{1 - \text{H}_2\text{O}_{mole \text{ fraction}}}$$

Figures 12 and 13 show the average NO_x ppm in the outlet of the system, either for WF and WA simulations.

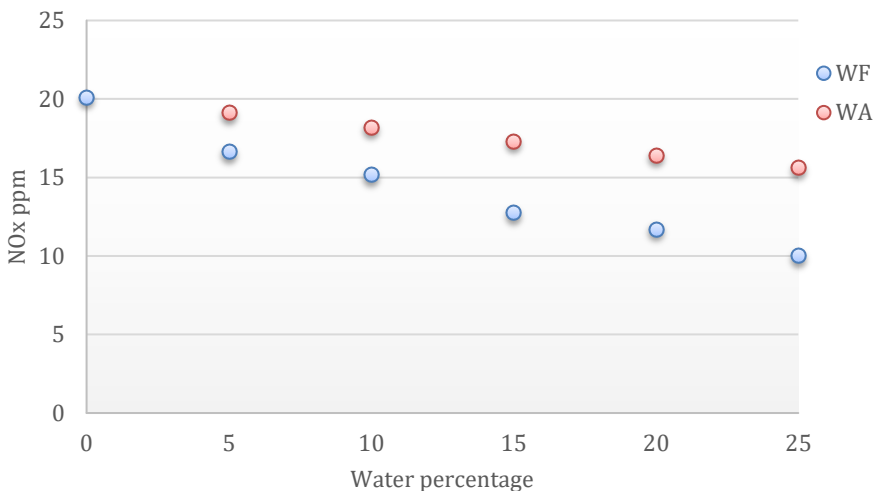


Figure 12: Biomethane average outlet NO_x ppm.

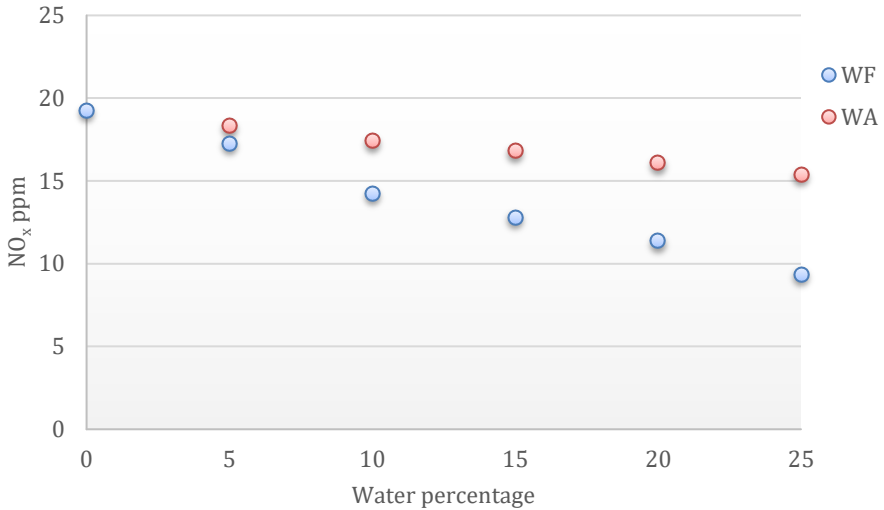


Figure 13: Methane average outlet NO_x ppm.

From the figures above, it is clear that the contact model influences the behavior of the system, as *Iglesias (2015)* observed in his final master thesis. However, the results of this study have some differences from the results obtained by *Iglesias (2015)*.

On the one hand, the difference between water in air and water in fuel is much smaller when comparing with the previous mentioned study. This is because the combustor of this project features a swirl that affects the air inlet, which conducts to a faster mixing of air and fuel, so that the contact model loses influence as seen in Figures 12 and 13.

On the other hand, it is observed that as water percentage increases, the difference between water in air and water in fuel becomes more notable. This is probably because the swirl only affects the air inlet, and when water percentage becomes important, swirl is not able to properly mix air and fuel. Furthermore, it is important to remember that fuel enters the chamber at around 160 m/s while air velocity inlet is about 32 m/s.

Finally, the last step before showing result profiles is to expose summary tables of the most important results that have been obtained. These results are seen in Tables 7 and 8.

Table 7. Biomethane results summary.

Inlet with water	Water percentage	Average NO_x ppm outlet	Temperature peak [K]	Average temperature outlet [K]
Dry case	0	20.12	2014.91	1431.23
Fuel	5	16.64	2003.50	1430.32
	10	15.18	1999.00	1429.11
	15	12.76	1988.78	1428.05
	20	11.71	1985.18	1426.92
	25	10.01	1976.92	1425.55
	Air	5	19.13	2011.45
10		18.20	2007.95	1429.90
15		17.29	2004.43	1429.25
20		16.43	2000.91	1428.60
25		15.62	1997.40	1427.95

Table 8. Methane results summary.

Inlet with water	Water percentage	Average NO_x ppm outlet	Temperature peak [K]	Average temperature outlet [K]
Dry case	0	19.27	1987.71	1468.31
Fuel	5	17.29	1981.33	1468.28
	10	14.25	1969.70	1468.15
	15	12.81	1964.14	1467.42
	20	11.39	1957.75	1466.77
	25	9.38	1946.42	1465.89
Air	5	18.32	1984.28	1467.64
	10	17.42	1980.91	1466.97
	15	16.82	1979.13	1466.46
	20	16.10	1976.45	1465.88
	25	15.39	1973.59	1465.24

From the tables above, it is seen that as the amount of water added increases, NO_x production and temperature in the system decrease. As explained before, water absorbs part of the heat produced in the combustion, allowing to reduce the system overall temperature. As the temperatures are in some cases above 2000 K, thermal NO_x is drastically reduced when reached temperature decreases, which is reflected in the NO_x ppm in the system outlet.

In the following subsections all the obtained profiles are shown, and an analysis and interpretation of them is done. First, biomethane profiles are provided from Figure 14 to Figure 17 and from Figure 22 to Figure 25, followed by industrial methane profiles, provided from Figure 18 to Figure 21 and from Figure 26 to Figure 29. Moreover, the first six profiles correspond to water in fuel cases while the next six profiles to water in air cases. The color scale is the same for all the graphics of the same kind, so that they can be easily compared.

7.1. TEMPERATURE PROFILES

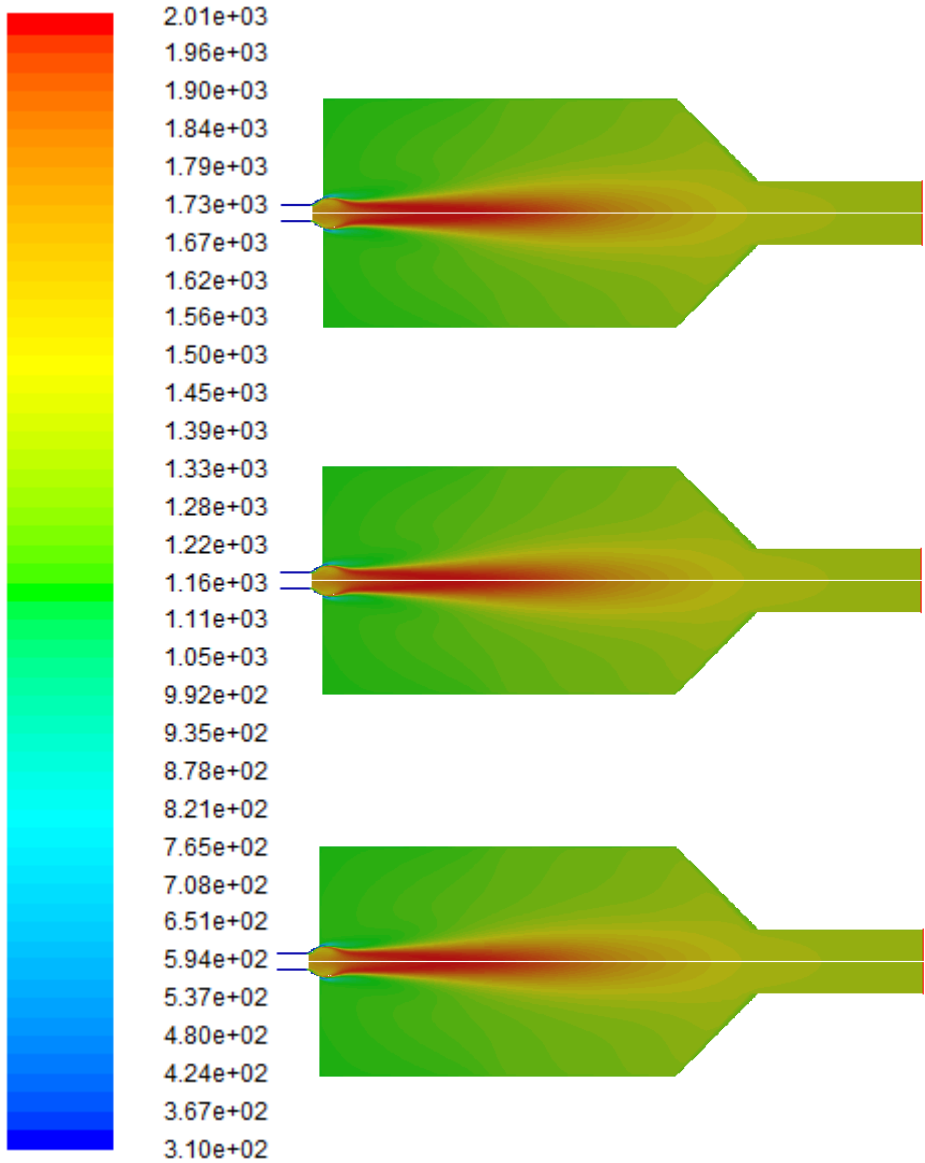


Figure 14: Biomethane temperature profiles. From up to down: 0%, 5% and 10% water in fuel.

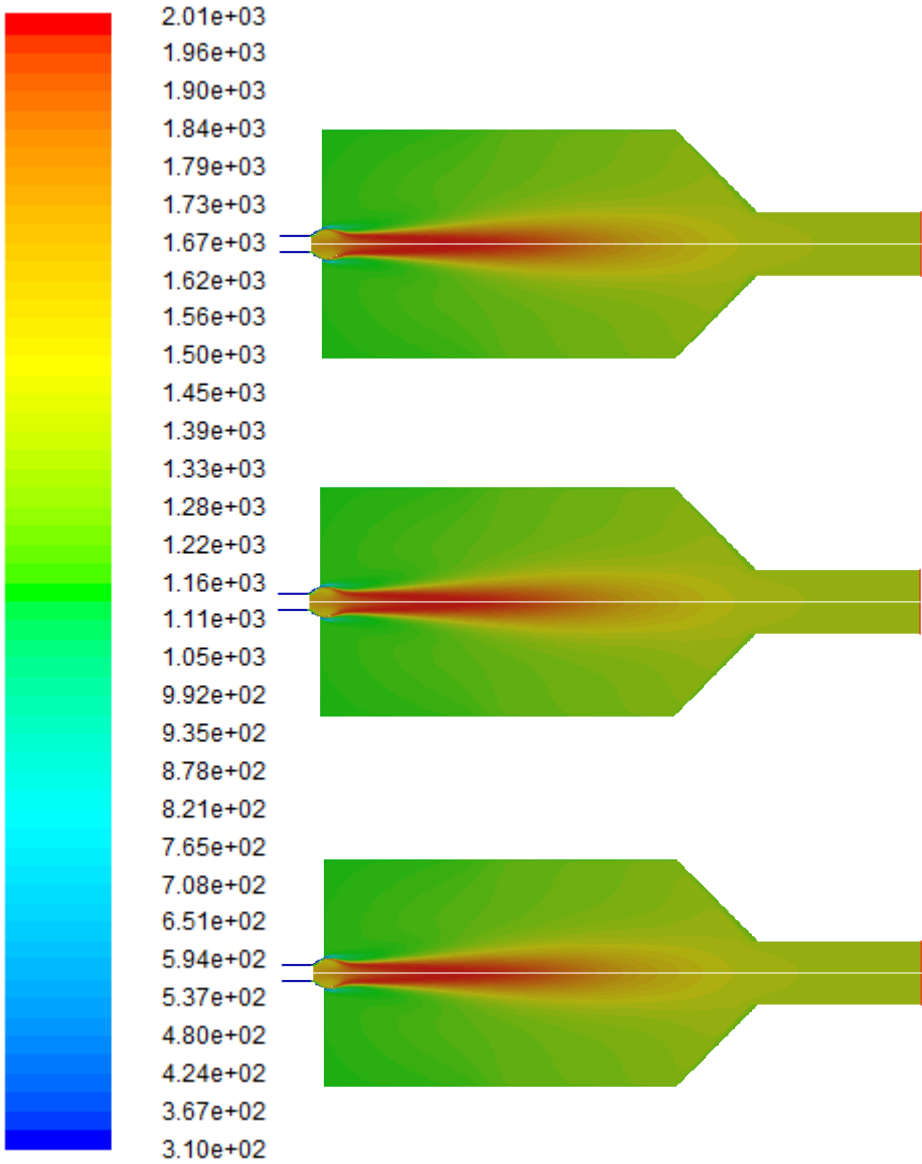


Figure 15: Biomethane temperature profiles. From up to down: 15%, 20% and 25% water in fuel.

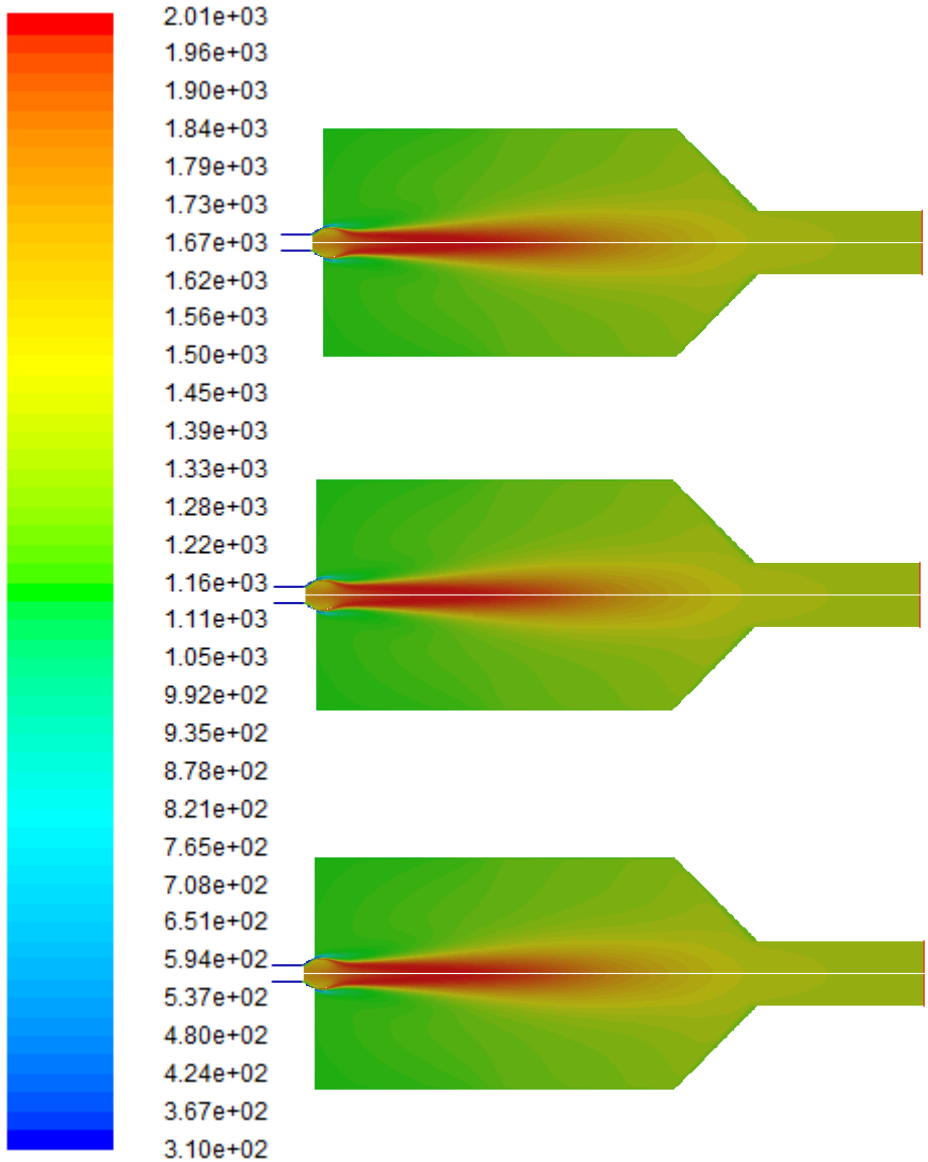


Figure 16: Biomethane temperature profiles. From up to down: 0%, 5% and 10% water in air.

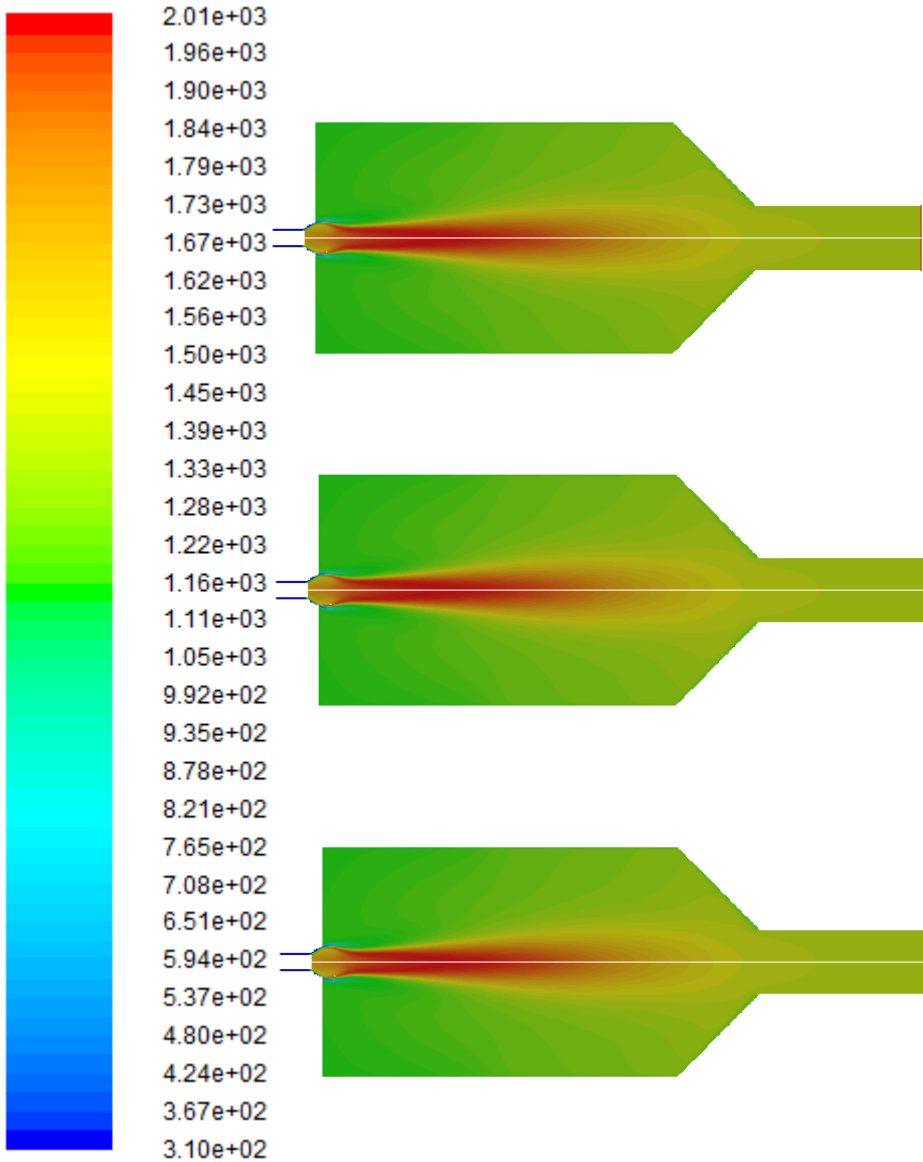


Figure 17: Biomethane temperature profiles. From up to down: 15%, 20% and 25% water in air.

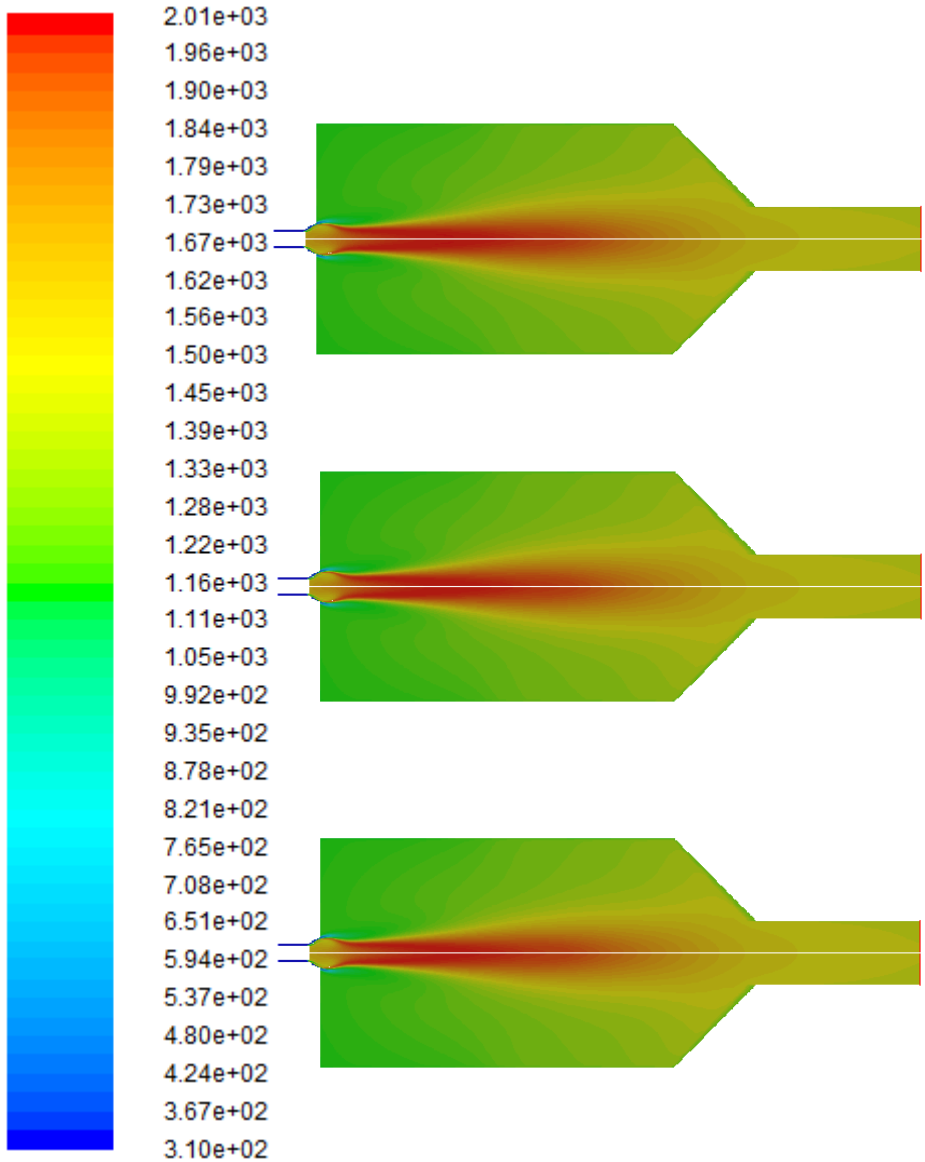


Figure 18: Methane temperature profiles. From up to down: 0%, 5% and 10% water in fuel.

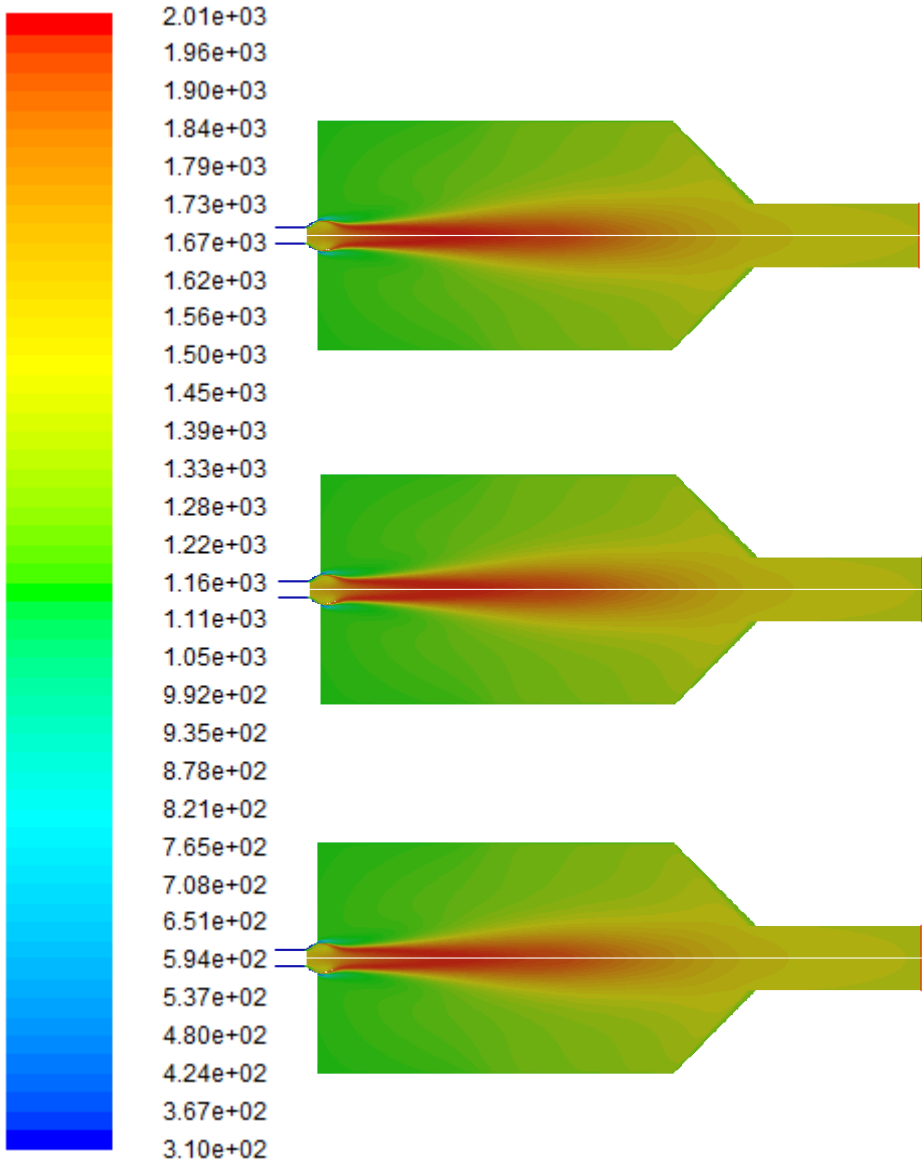


Figure 19: Methane temperature profiles. From up to down: 15%, 20% and 25% water in fuel.

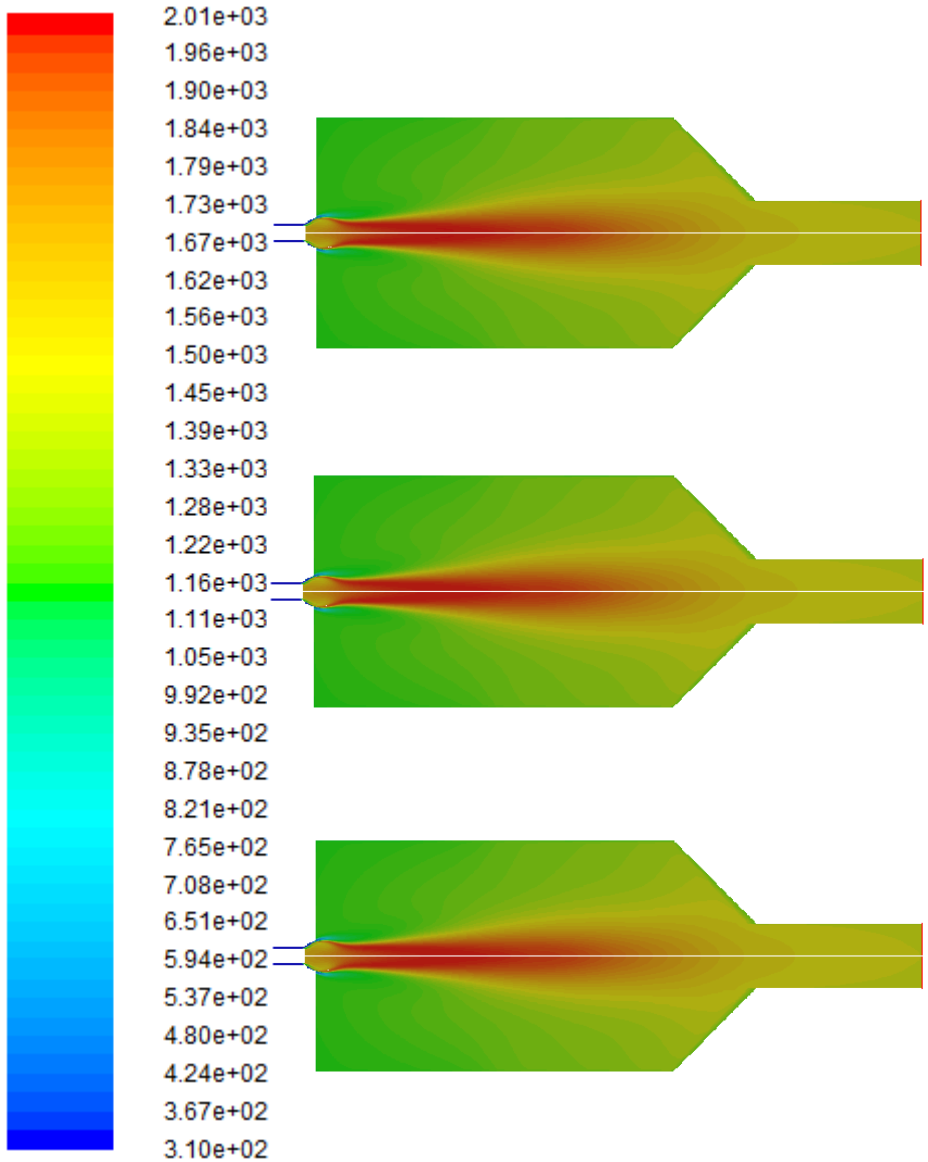


Figure 20: Methane temperature profiles. From up to down: 0%, 5% and 10% water in air.

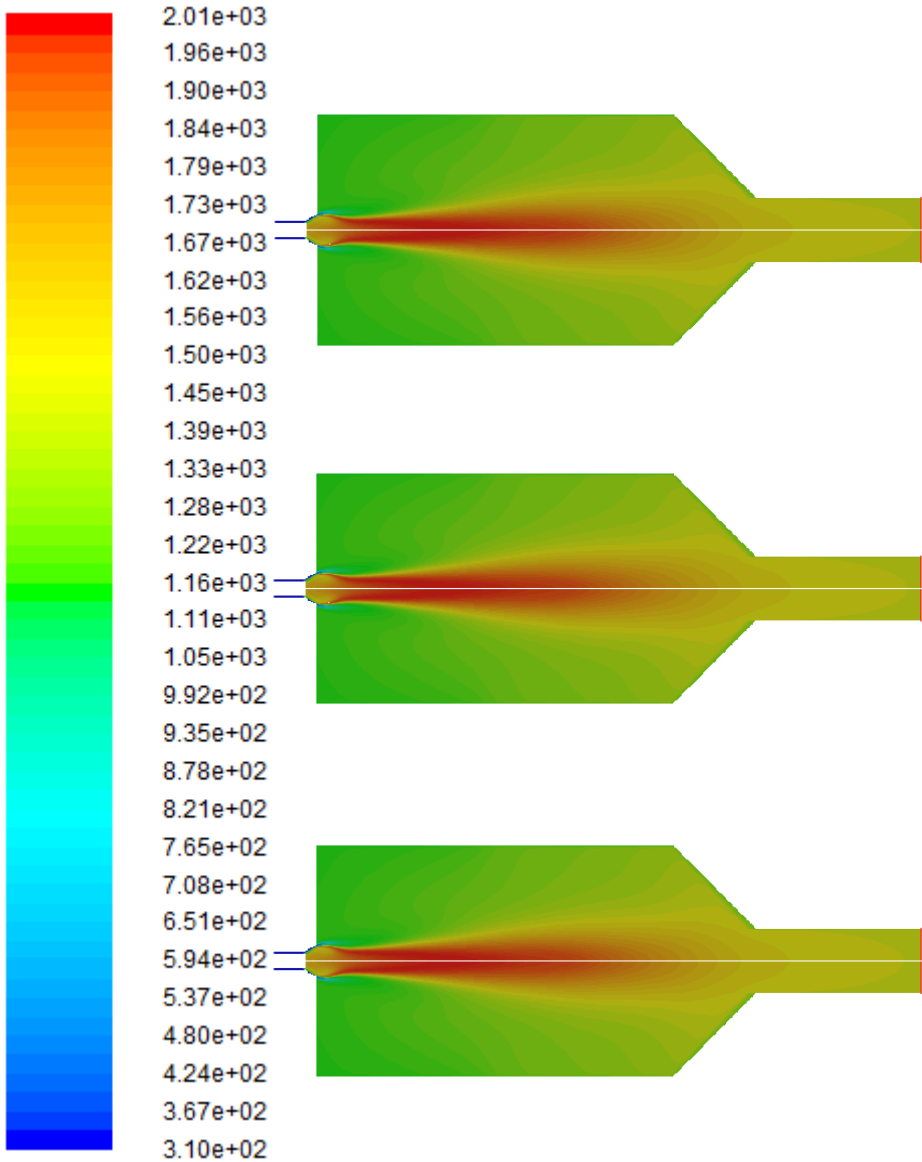


Figure 21: Methane temperature profiles. From up to down: 15%, 20% and 25% water in air.

It is observed that as predicted a few sections before, combustion takes place around the symmetry axis, and thus the most important changes in system properties are made in this zone. This means that the mesh refinement explained before has been done in the right zone of the system, and it has allowed to obtain more accurate results while calculation time is still reasonable.

Moreover, although these contours might seem similar, values of peak temperature and average outlet temperature change from one case to another. Graphics look very similar because the scale covers a wide range of temperatures (from 310 K to 2010 K approximately), which means that temperature must change a lot to see differences between them. However, taking into account that when temperature is around 2000 K, the amount of NO_x produced doubles every 90 K, a small difference in peak temperature can have a very important effect in NO_x formation, as seen in the next section.

As shown in Tables 7 and 8, when water is added to fuel, temperature reduction is more important than when the addition is made in the air. Furthermore, as seen from the graphics, the difference between methane and biogas is almost null in terms of reached temperature, which means that biogas could give approximately the same energy when combusted that methane or natural gas, but being a renewable energy and not a fossil fuel.

The following section includes the NO_x ppm profiles obtained during the simulations. They are presented in the same order as temperature profiles, and they illustrate the effect of temperature decrease in NO_x formation due to water addition.

7.2. NO_x PPM PROFILES

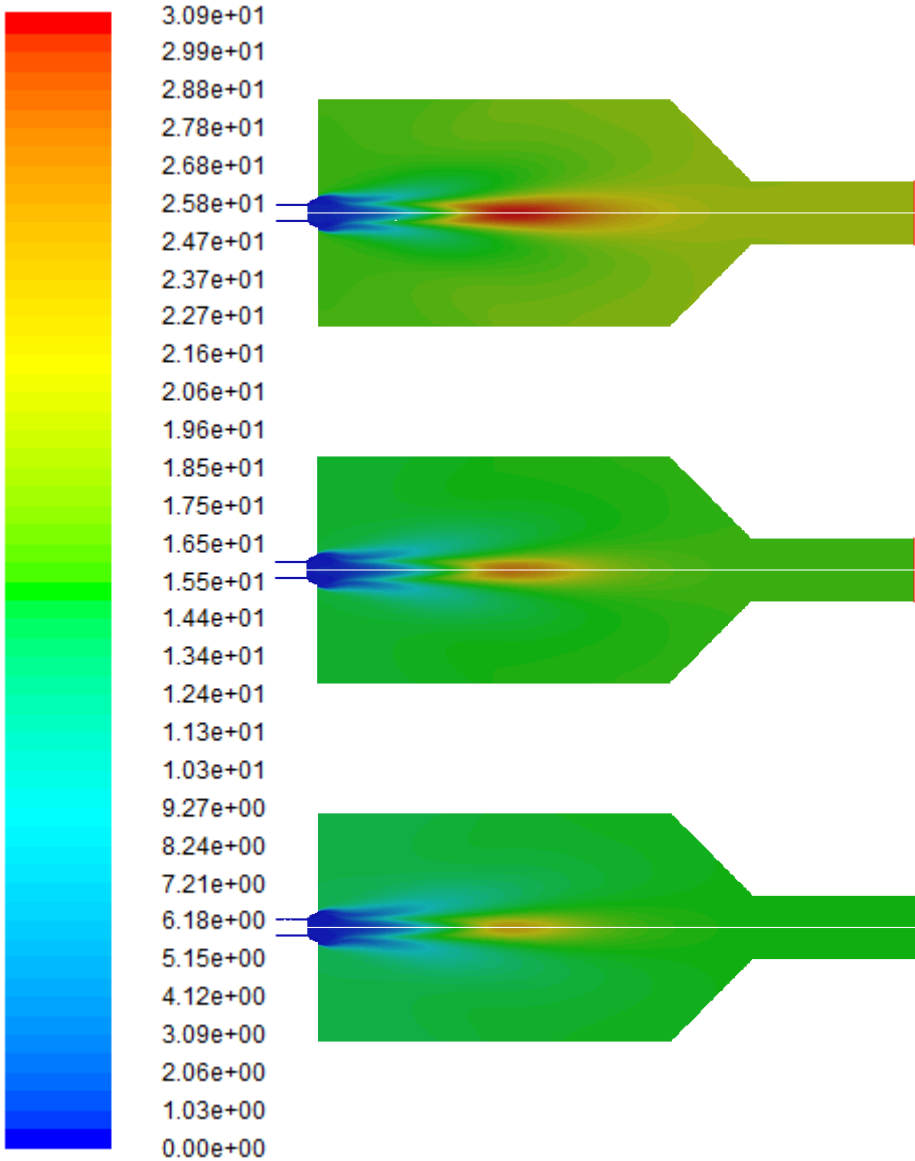


Figure 22: Biomethane NO_x ppm profiles. From up to down: 0%, 5% and 10% water in fuel.

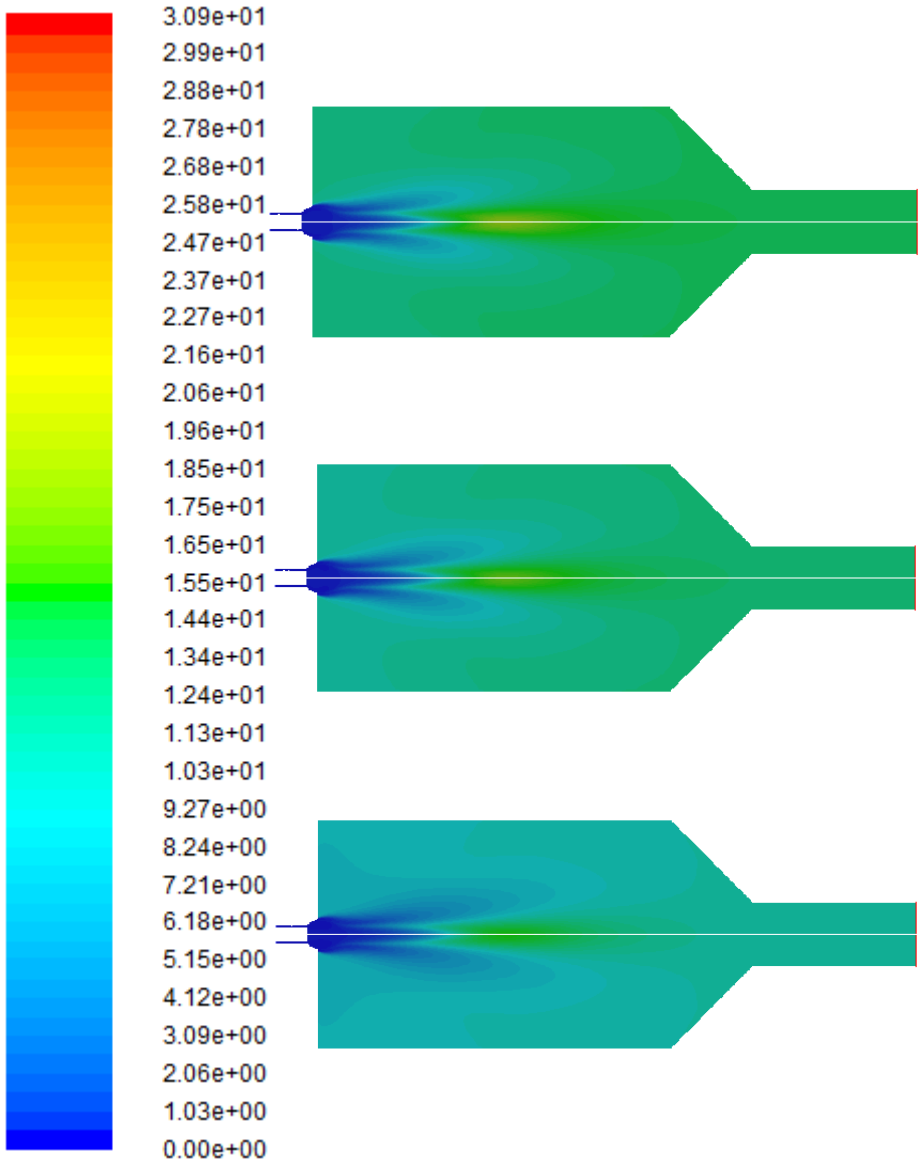


Figure 23: Biomethane NO_x ppm profiles. From up to down: 15%, 20% and 25% water in fuel.

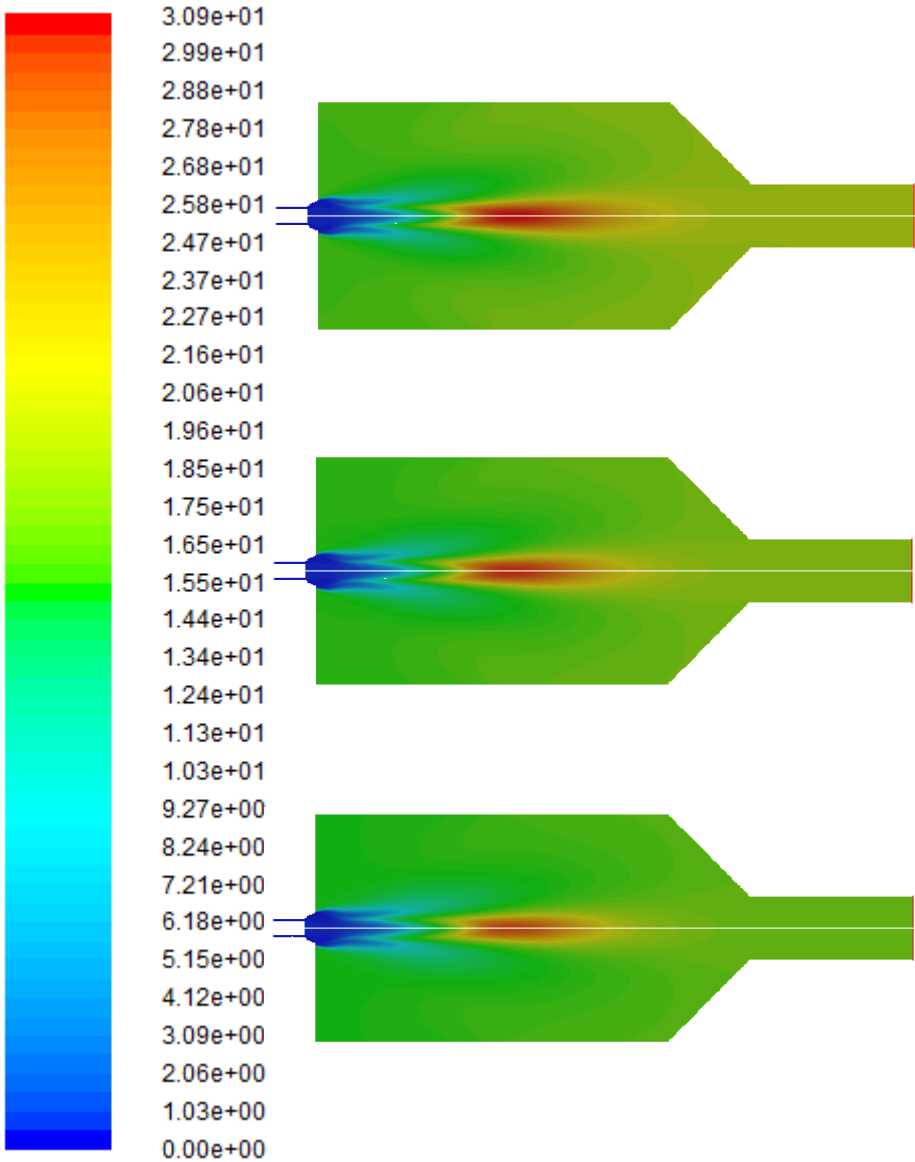


Figure 24: Biomethane NO_x ppm profiles. From up to down: 0%, 5% and 10% water in air.

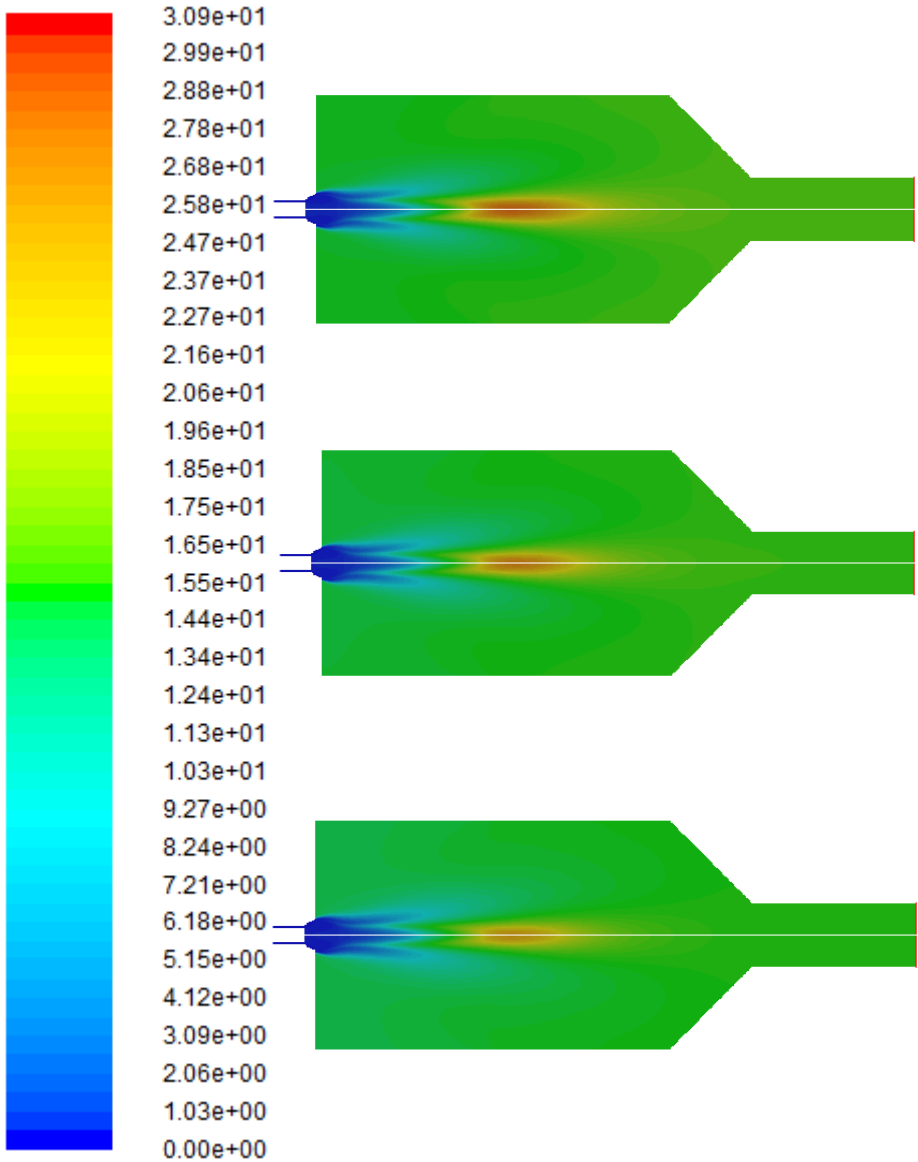


Figure 25: Biomethane NO_x ppm profiles. From up to down: 15%, 20% and 25% water in air.

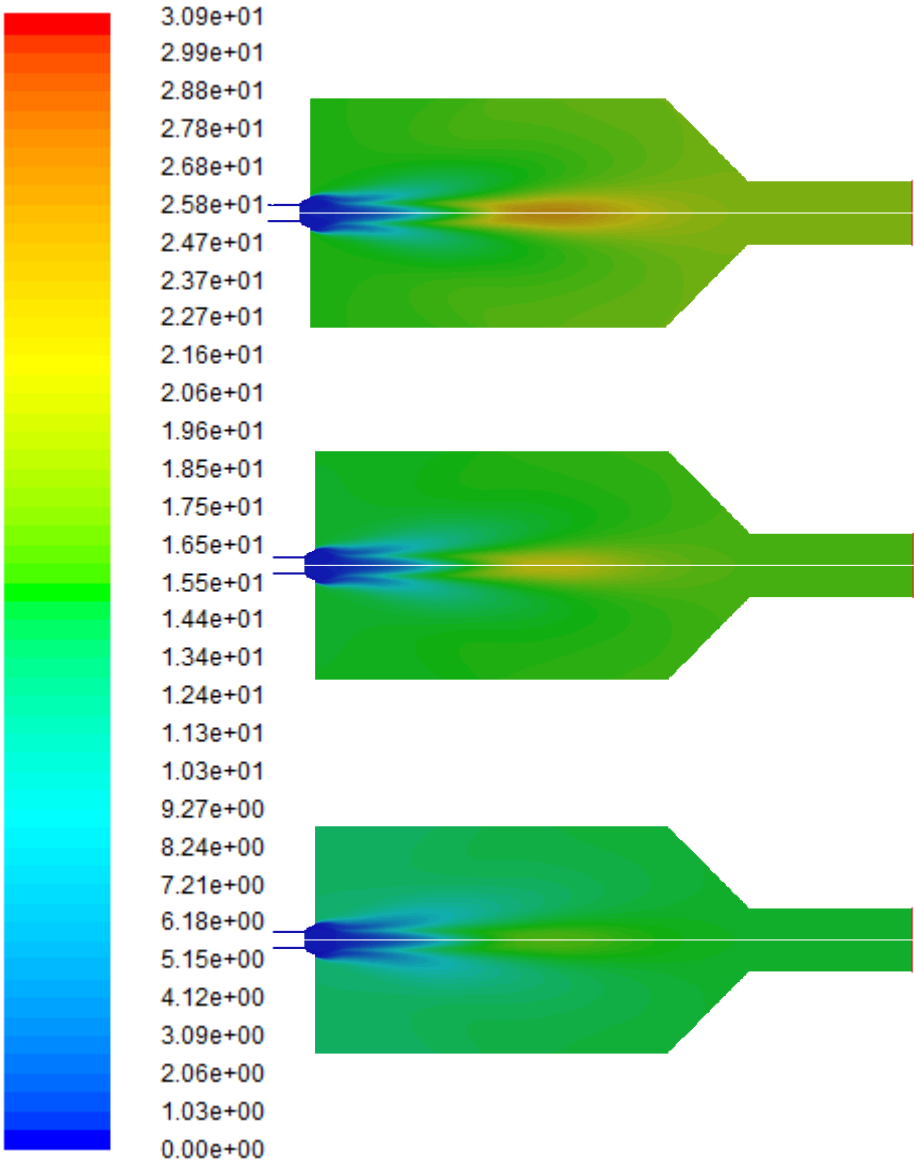


Figure 26: Methane NO_x ppm profiles. From up to down: 0%, 5% and 10% water in fuel.

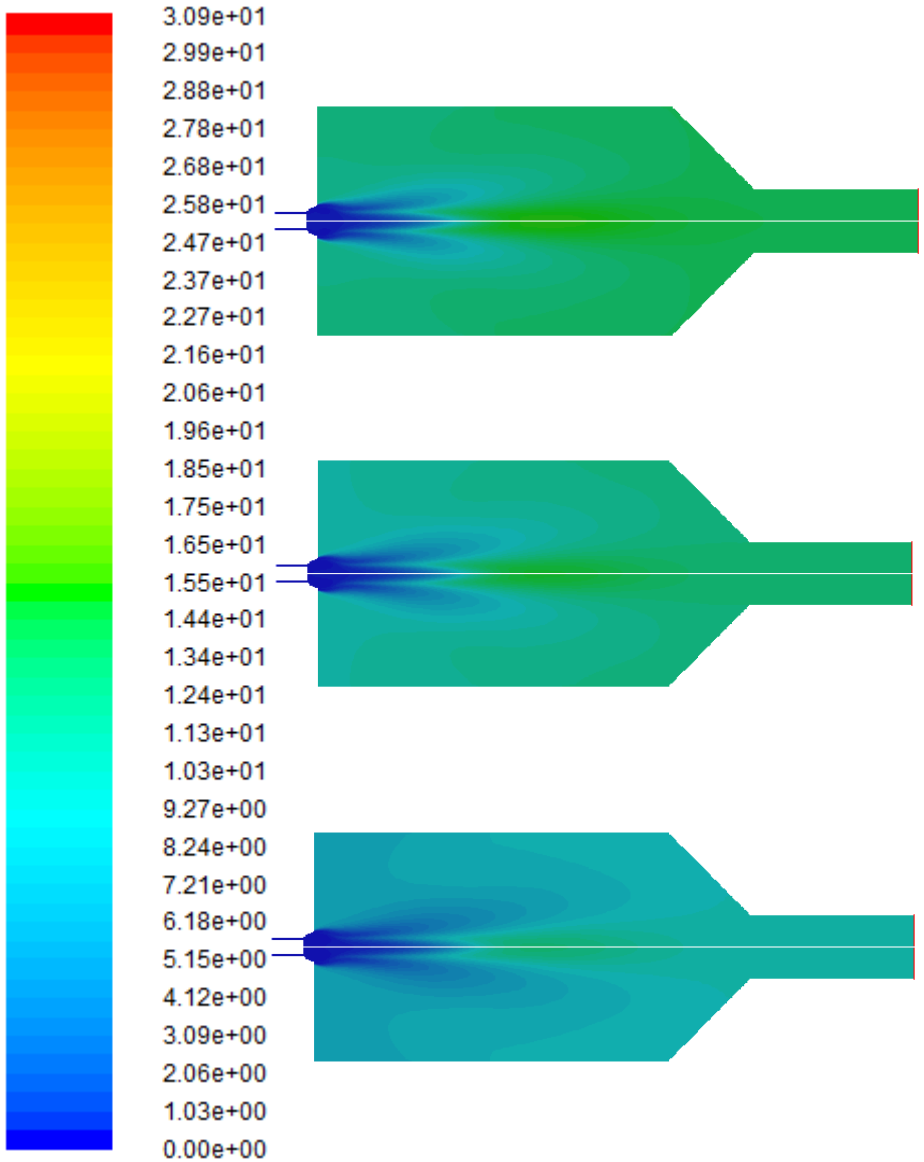


Figure 27: Methane NO_x ppm profiles. From up to down: 15%, 20% and 25% water in fuel.

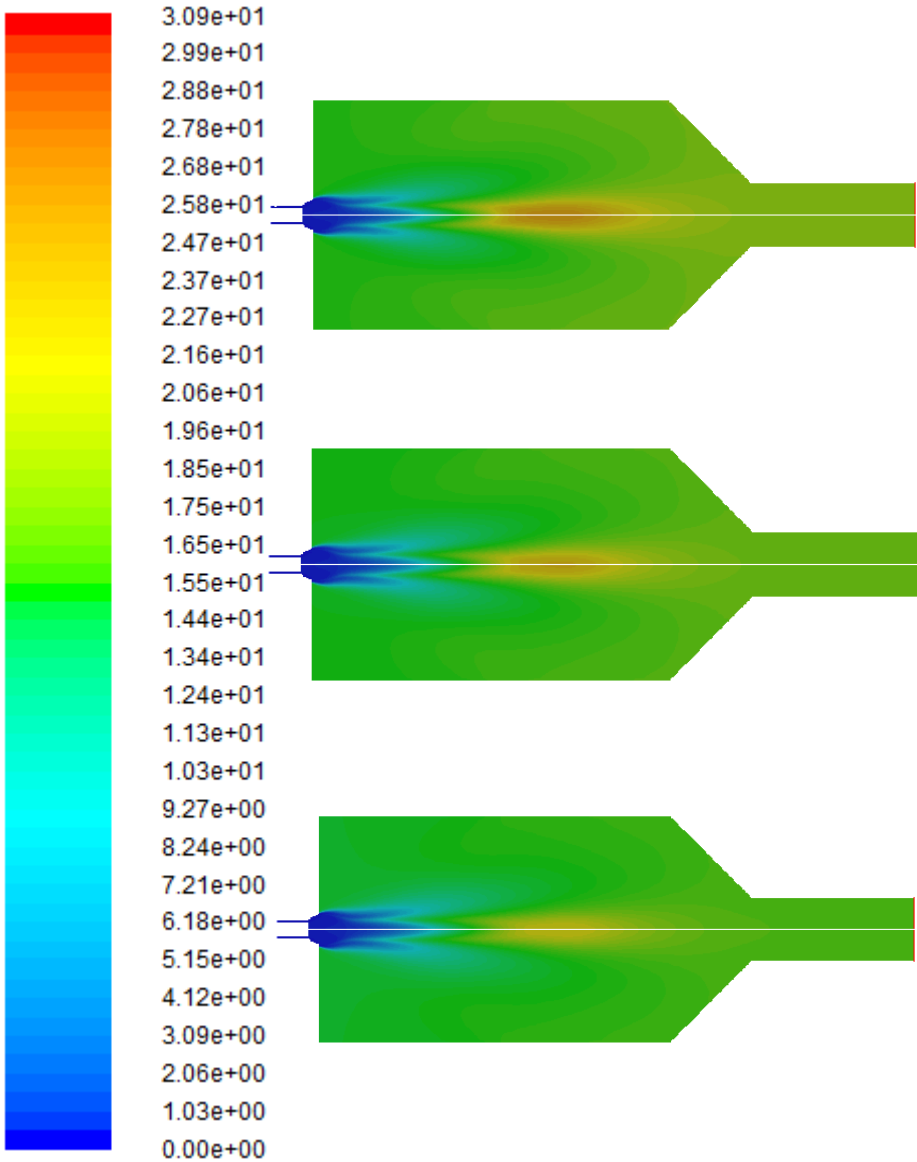


Figure 28: Methane NO_x ppm profiles. From up to down: 0%, 5% and 10% water in air.

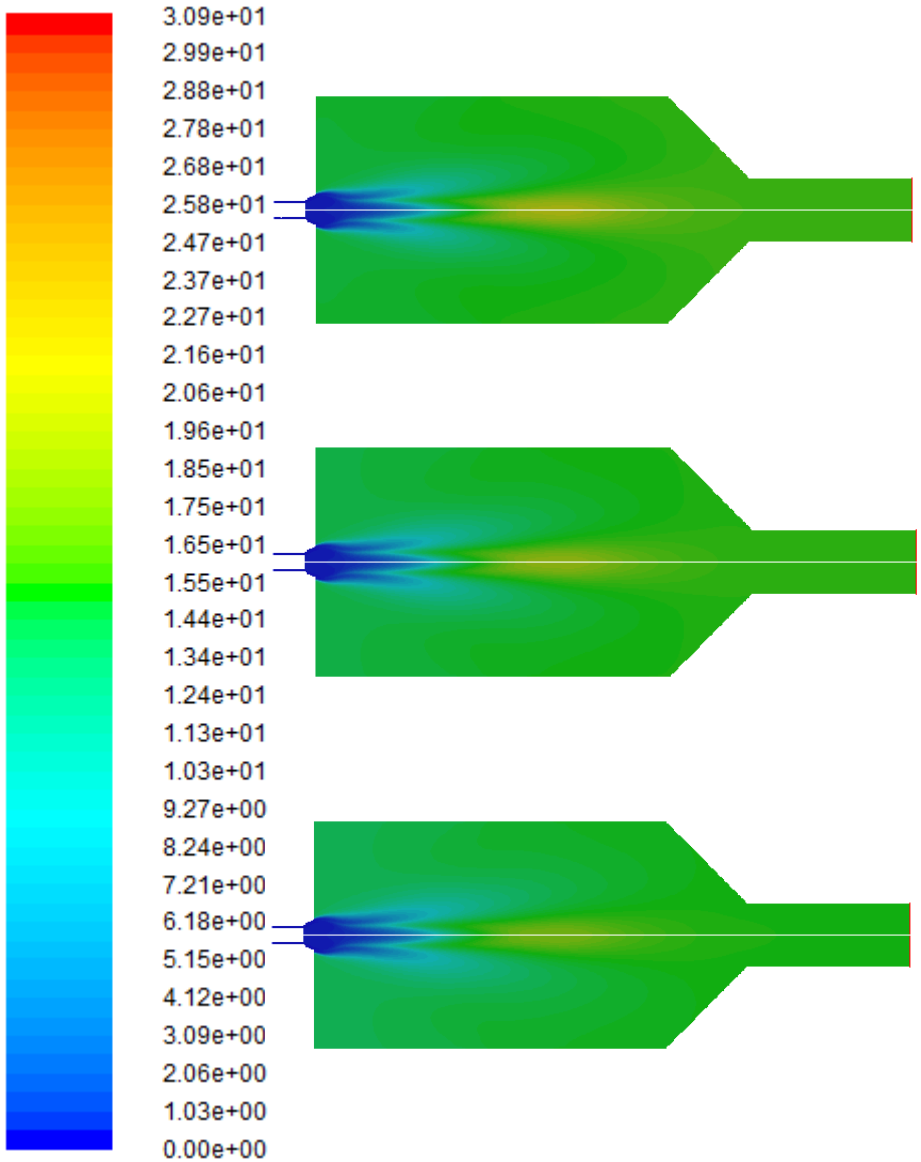


Figure 29: Methane NO_x ppm profiles. From up to down: 15%, 20% and 25% water in air.

It is observed that water addition has a very important impact in terms of NO_x formation. The difference between graphics is quite large, and NO_x production almost halves in comparison with the dry case. As commented before, although peak temperature difference is around 40 K between the dry case and the 25% water in fuel case, the effect in NO_x rate production is much bigger than could be expected.

Once more, in these graphics it is seen that the water addition effect is more important when it is added to the fuel than to the air, and also the most important changes are around the symmetry axis. NO_x ppm peak is in the same zone that peak temperature is, which has logic taking into account that thermal NO_x formation is more important as temperature increases, because chemical reactions that involve it highly depend on temperature.

According to Tables 7 and 8, methane average NO_x ppm outlet is slightly less than biomethane, but the difference is almost negligible (less than 1 ppm). Keeping in mind that biogas is a renewable energy while methane and natural gas are fossil fuels, it would be advisable to start to replace them in order to generate energy in a more sustainable way.

8. CONCLUSIONS

The most remarkable conclusion is that NO_x ppm production is less than half while outlet temperature is barely 5 K lower when comparing the 25% water in fuel case with the dry case. This is very important, because it means that almost the same energy could be produced with a lower environmental cost.

Moreover, it is observed that the contact model influences both the pollutant formation and the energy produced, as seen in Figures 12 and 13. It is interesting, because having exactly the same quantities of fuel, air and water in the combustion chamber, the obtained results are different. This illustrates how important is the contact model, and that it has to be taken into account when performing any chemical reaction.

However, if compared with *Iglesias (2015)* final master thesis, it is observed that the contact model has less influence in this study. The reason is that the swirl that this combustion chamber features mixes the fuel and the air so fast that the contact model losses influence when comparing with a non-swirl experiment. In fact, it is not that the contact model loses influence, but that the contact model changes due to swirl presence in the system.

Furthermore, from the comparison between biomethane and industrial methane, it is observed that NO_x production is slightly lower in industrial methane than in biomethane. However, the difference is less than 1 ppm, and given that biomethane is a renewable energy while industrial methane is a fossil fuel, it could be worth to start using biomethane to replace fossil fuels in order to produce energy in a more sustainable way.

Finally, to understand better why NO_x production has experience such an important decrease due to water addition, more graphics are shown in the Appendices. As explained before, in this study two mechanisms of NO_x formation are used: thermal NO_x formation and prompt NO_x formation. By illustrating its profiles, it is possible to see which varies the most, and based on the results, one can see which factor contributes the most in this reduction, in order to make possible further improvements.

9. REFERENCES AND NOTES

1. M. M. Noor; Andrew P.Wandel¹; Talal Yusaf. Detail guide for CFD on the Simulation of Biogas Combustion in Bluff-Body Mild Burner. International Conference on Mechanical Engineering Research. July **2013**. Paper ID: P342.
2. Rasi, Saija Emilia. Biogas composition and upgrading to biomethane. Jyväskylä: University of Jyväskylä, **2009**, p 43.
3. Latha, S., Borman, D. J. and Sleigh, P. A. CFD multiphase modelling for evaluation of gas mixing in an anaerobic digester. In: Aqua-enviro, TT, (ed.), 14th European Biosolids and Organic Resources Conference and Exhibition, 9-11th November **2009**, The Royal Armouries, Leeds, UK.
4. Leszek Chybowski; Rafal Laskowski; Katarzyna Gawdzinska. An overview of systems supplying water into the combustion chamber of diesel engines to decrease the amount of nitrogen oxides in exhaust gas. Japan society of Naval Architects and Ocean Engineers-Journal, January **2015** Review.
5. Thoharudin, Arif Setyo Nugroho, Edy Suryono. Computational Fluid Dynamics Simulation: Hydrogen Production from Biogas Autothermal in Monolithic Catalyst Reactor. Conference and Exhibition Indonesia – New, Renewable Energy and Energy Conservation (The 3rd Indo-EBTKE ConEx **2014**).
6. Iglesias, José Manuel. Study of Combustion Using Computational Fluid Dynamics Software (ANSYS). Final Master Thesis. University of Barcelona, February **2015**.
7. ANSYS Tutorial (2015); ANSYS FLUENT Tutorial guide. ANSYS, Inc. Release: 16.0, January **2015**.
8. ANSYS Theory (2015) ANSYS FLUENT Theory guide. ANSYS, Inc. Release: 16.2, July **2015**.
9. BMW. http://www.m-power.com/_open/s/editorial.jsp?id=3375&lang=en (BMW M4 GTS Water injection system). Visited April **2016**.
10. Union Gas Ltd. <https://www.uniongas.com/about-us/about-natural-gas/Chemical-Composition-of-Natural-Gas> (Information about industrial methane composition). Visited May **2016**.
11. United States Air Force. <https://www.airforce.com/> (Information about wet takeoff performed by Boeing KC-135). Visited May **2016**.

10. ACRONYMS

CFD	Computational Fluid Dynamics
NO _x	Mono-Nitrogen Oxides (NO and NO ₂)
SO _x	Sulfur Oxides
CHP	Combined Heat and Power
VOC	Volatile Organic Compound
MILD	Moderate and Intense Low oxygen Dilution
WF	Water in Fuel
WA	Water in Air

APPENDICES

APPENDIX 1: THERMAL NO_x RATE PROFILES

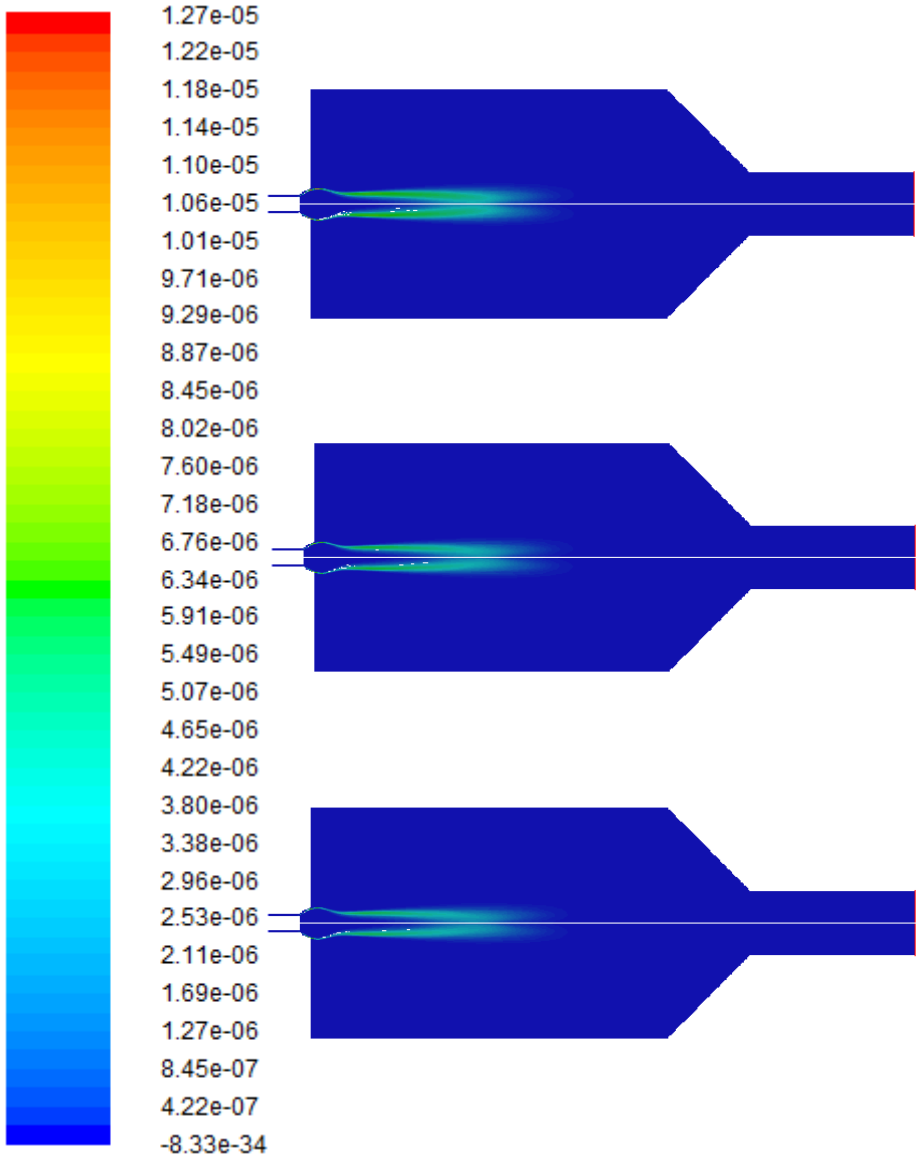


Figure 30: Biomethane thermal NO_x rate profiles. From up to down: 0%, 5% and 10% water in fuel.

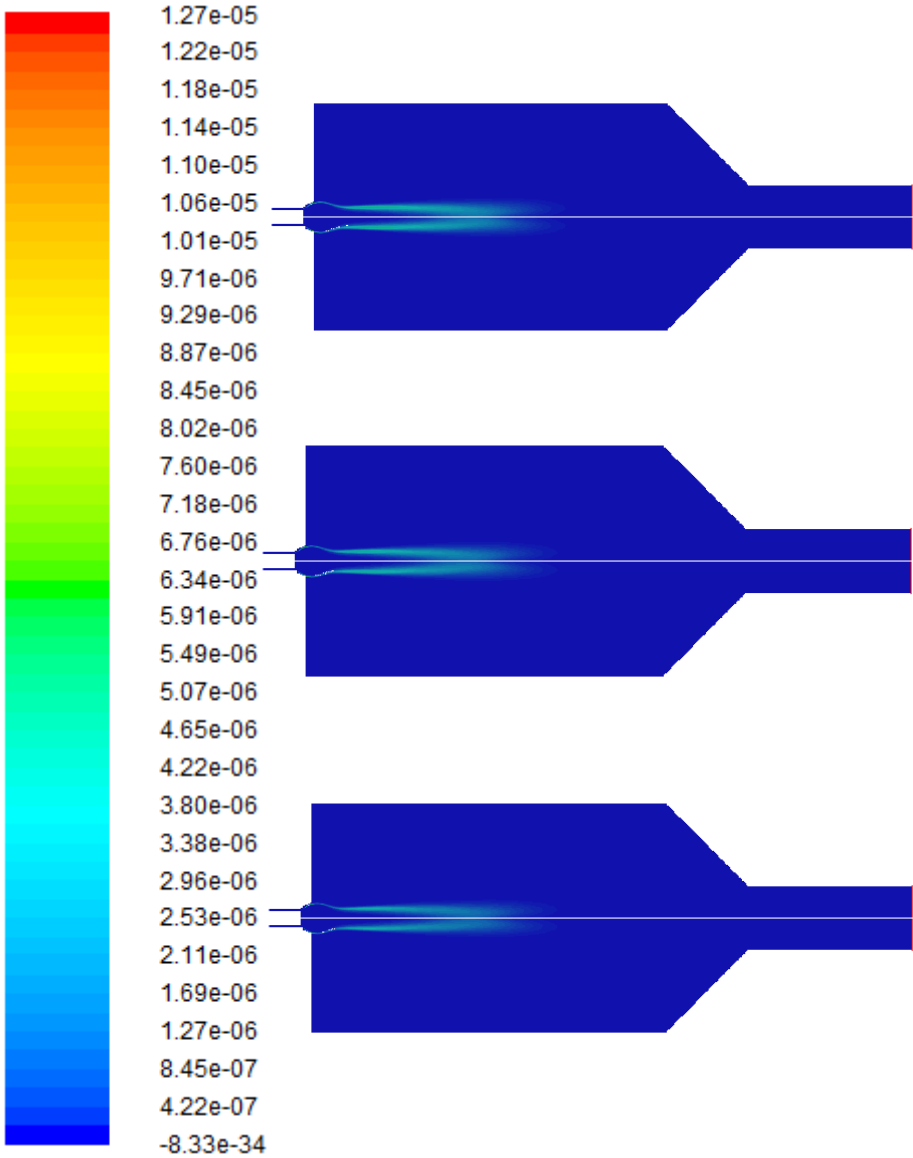


Figure 31: Biomethane thermal NO_x rate profiles. From up to down: 15%, 20% and 25% water in fuel.

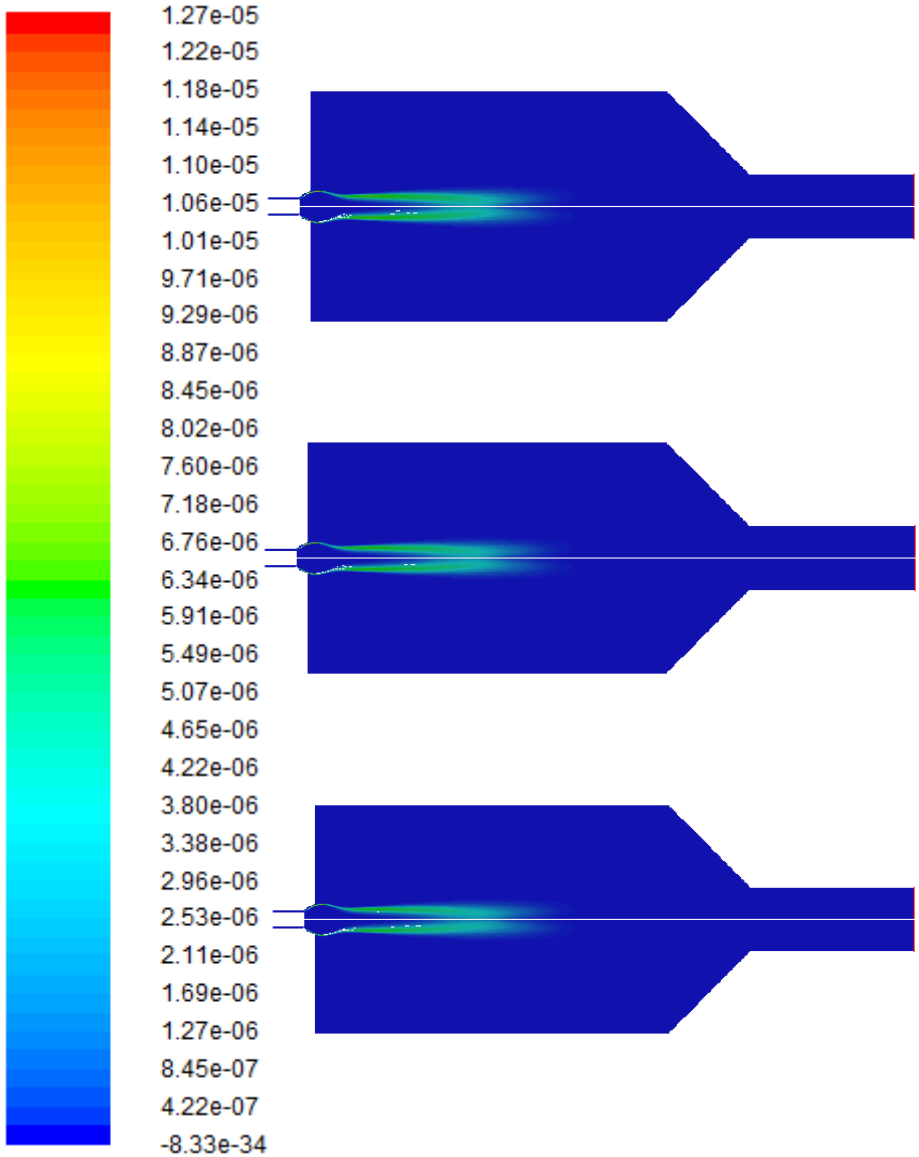


Figure 32: Biomethane thermal NO_x rate profiles. From up to down: 0%, 5% and 10% water in air.

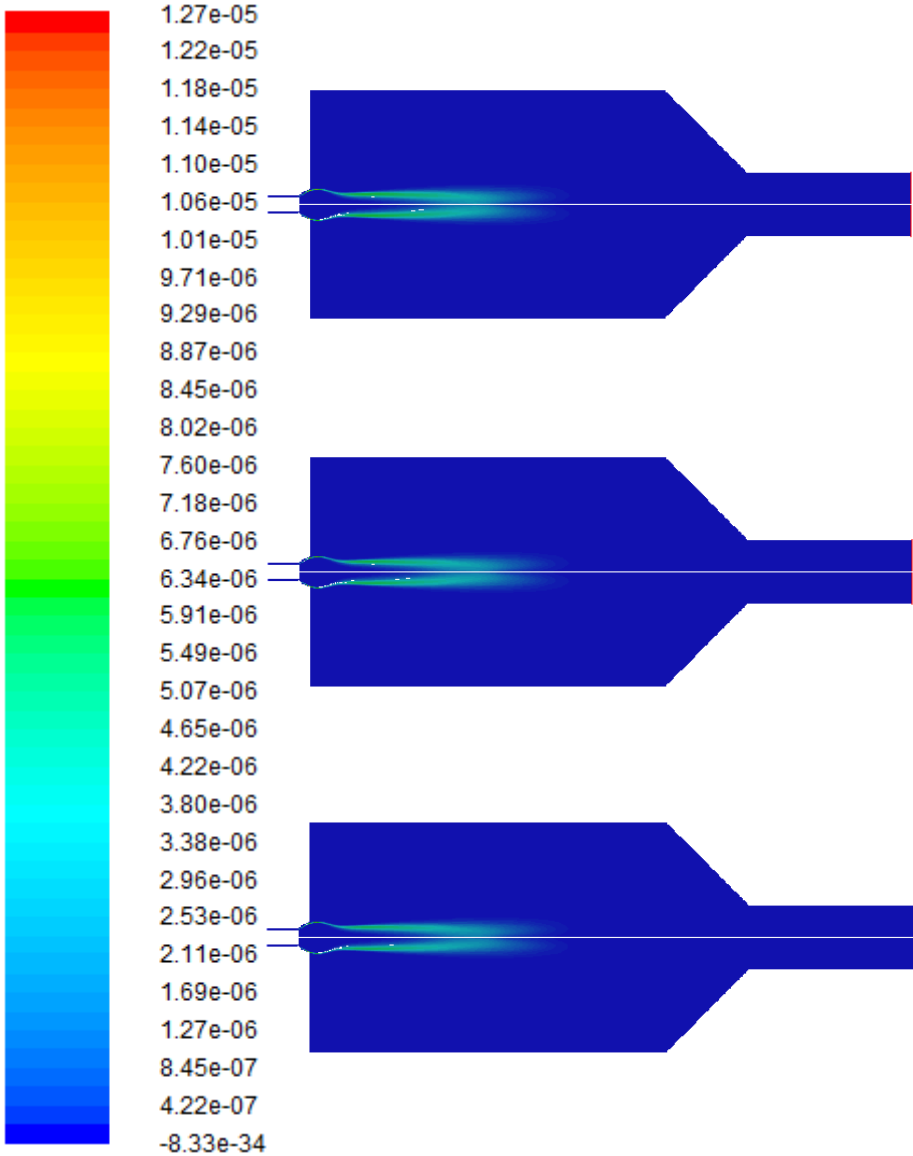


Figure 33: Biomethane thermal NO_x rate profiles. From up to down: 15%, 20% and 25% water in air.

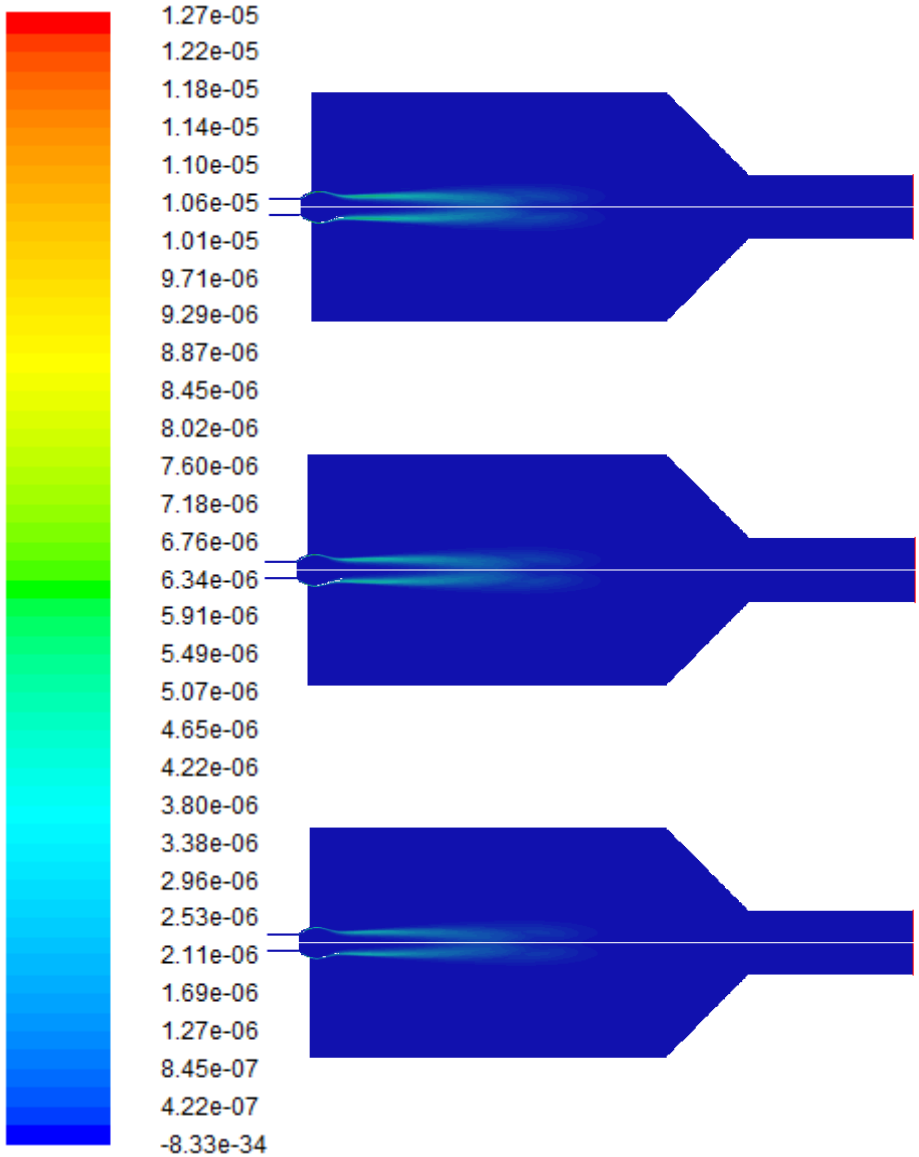


Figure 34: Methane thermal NO_x rate profiles. From up to down: 0%, 5% and 10% water in fuel.

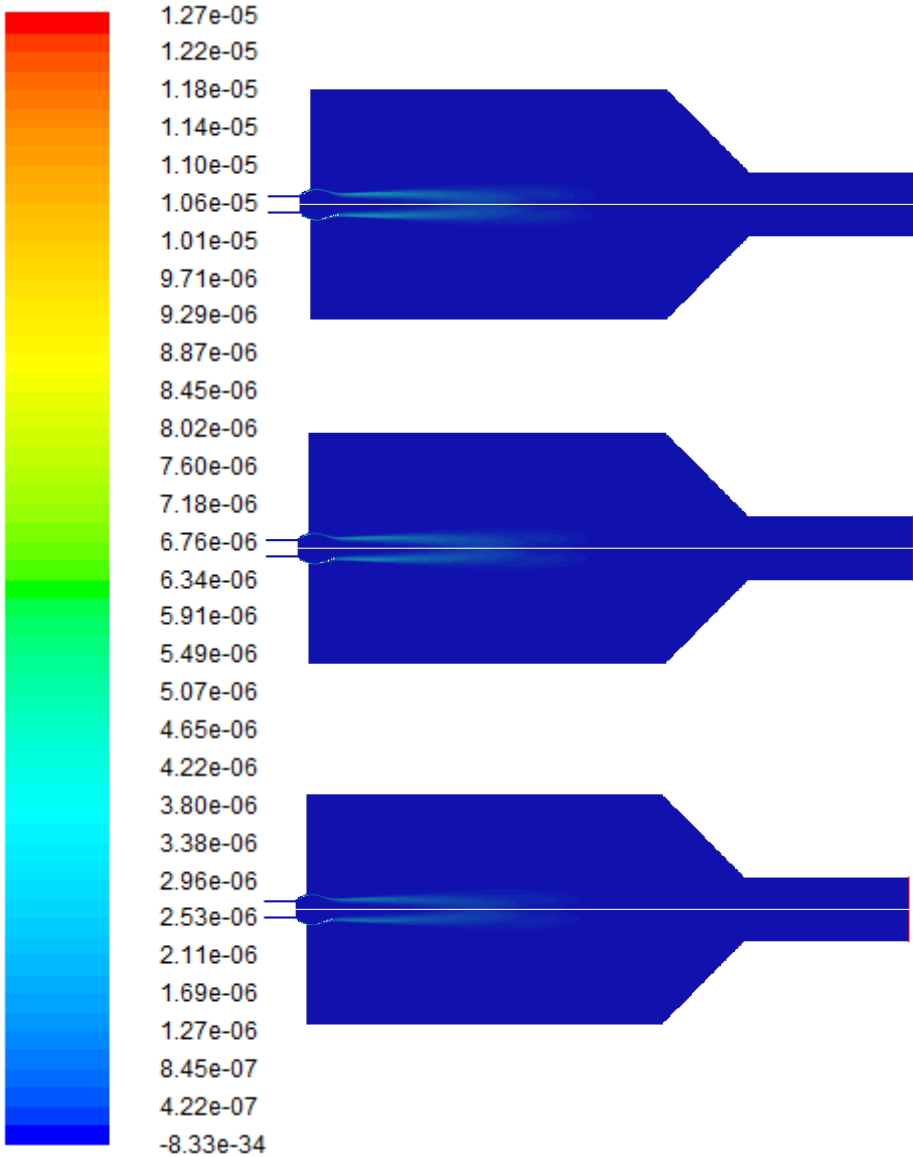


Figure 35: Methane thermal NO_x rate profiles. From up to down: 15%, 20% and 25% water in fuel.

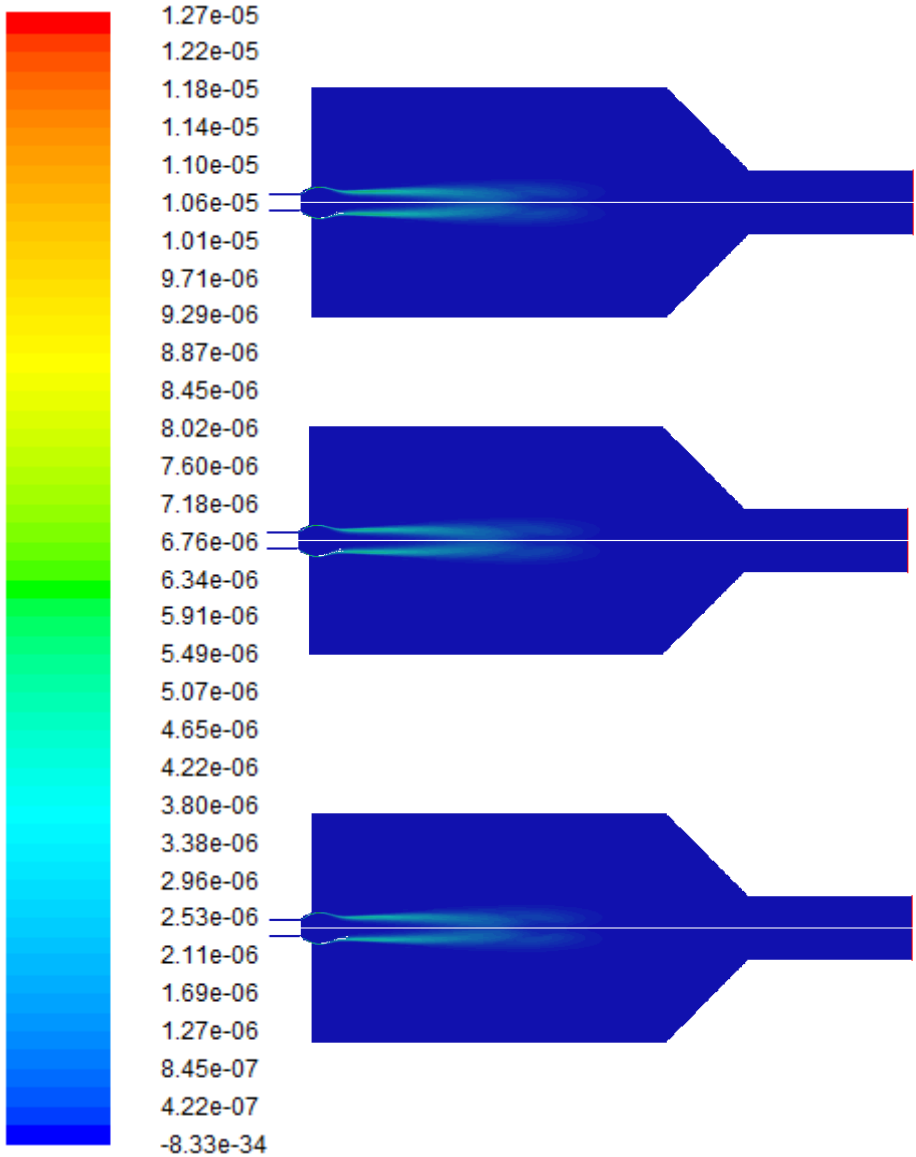


Figure 36: Methane thermal NO_x rate profiles. From up to down: 0%, 5% and 10% water in air.

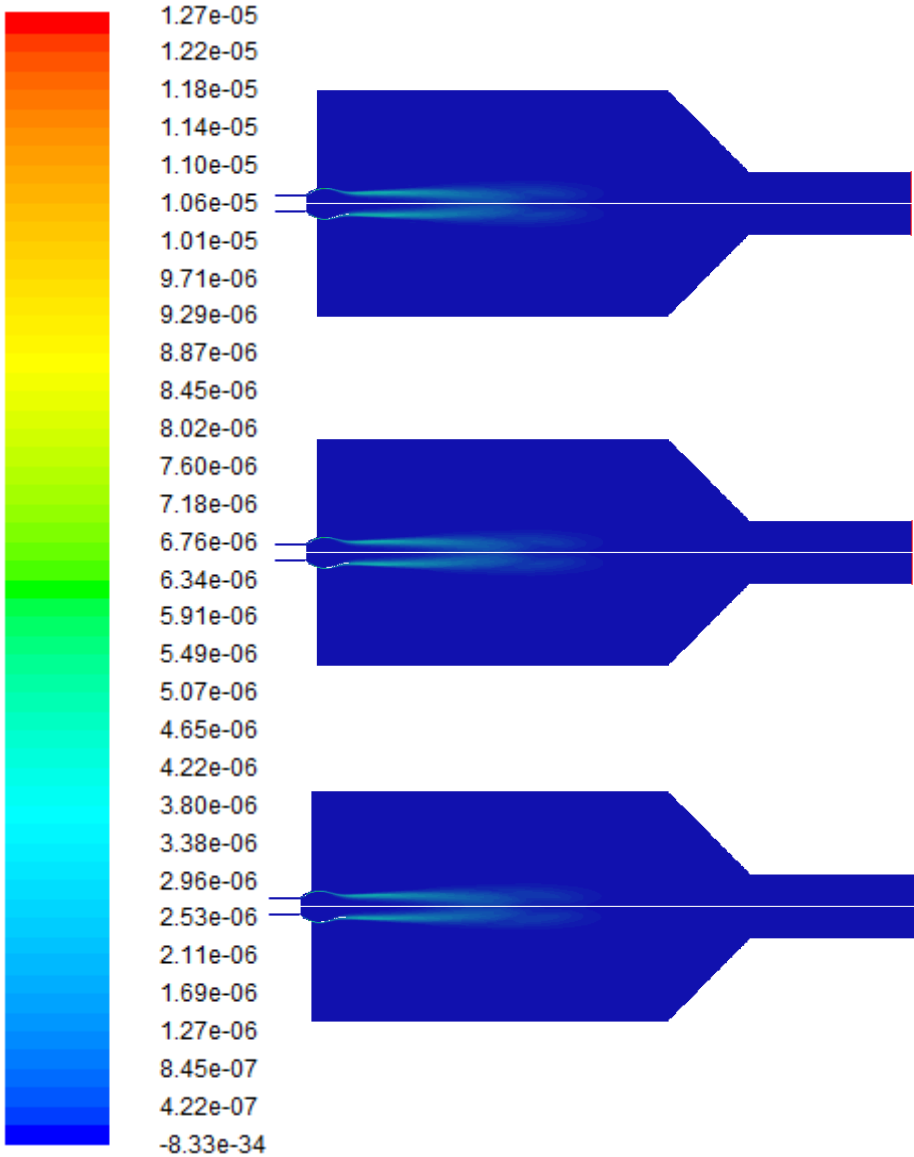


Figure 37: Methane thermal NO_x rate profiles. From up to down: 15%, 20% and 25% water in air.

APPENDIX 2: PROMPT NO_x RATE PROFILES

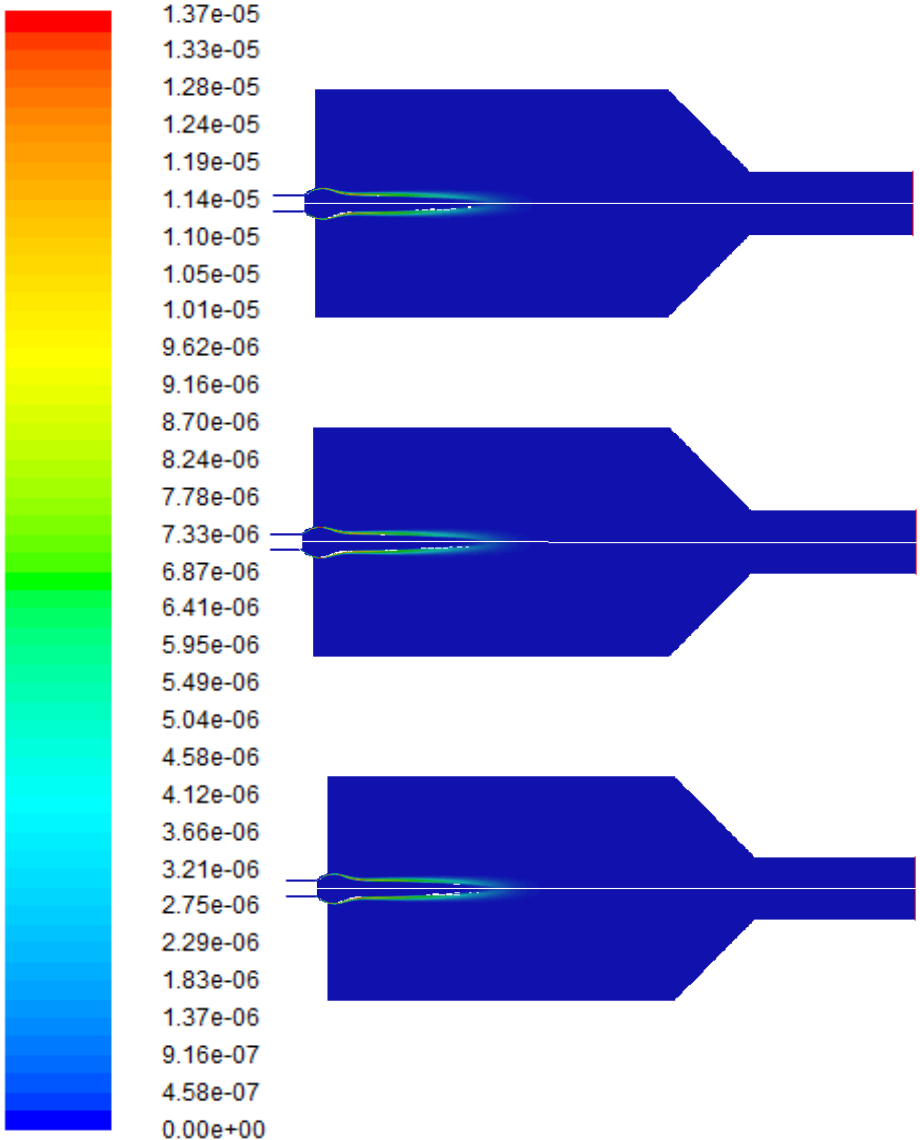


Figure 38: Biomethane prompt NO_x rate profiles. From up to down: 0%, 5% and 10% water in fuel.

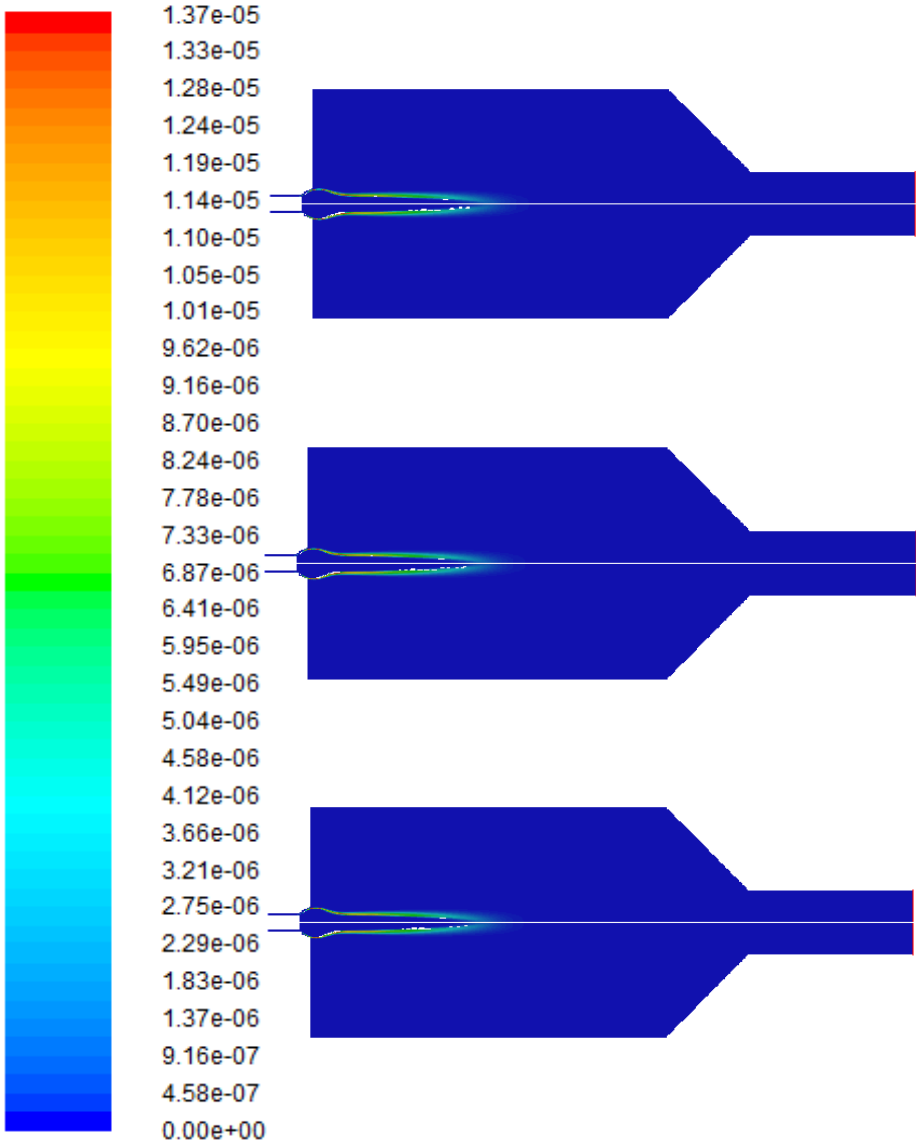


Figure 39: Biomethane prompt NO_x rate profiles. From up to down: 15%, 20% and 25% water in fuel.

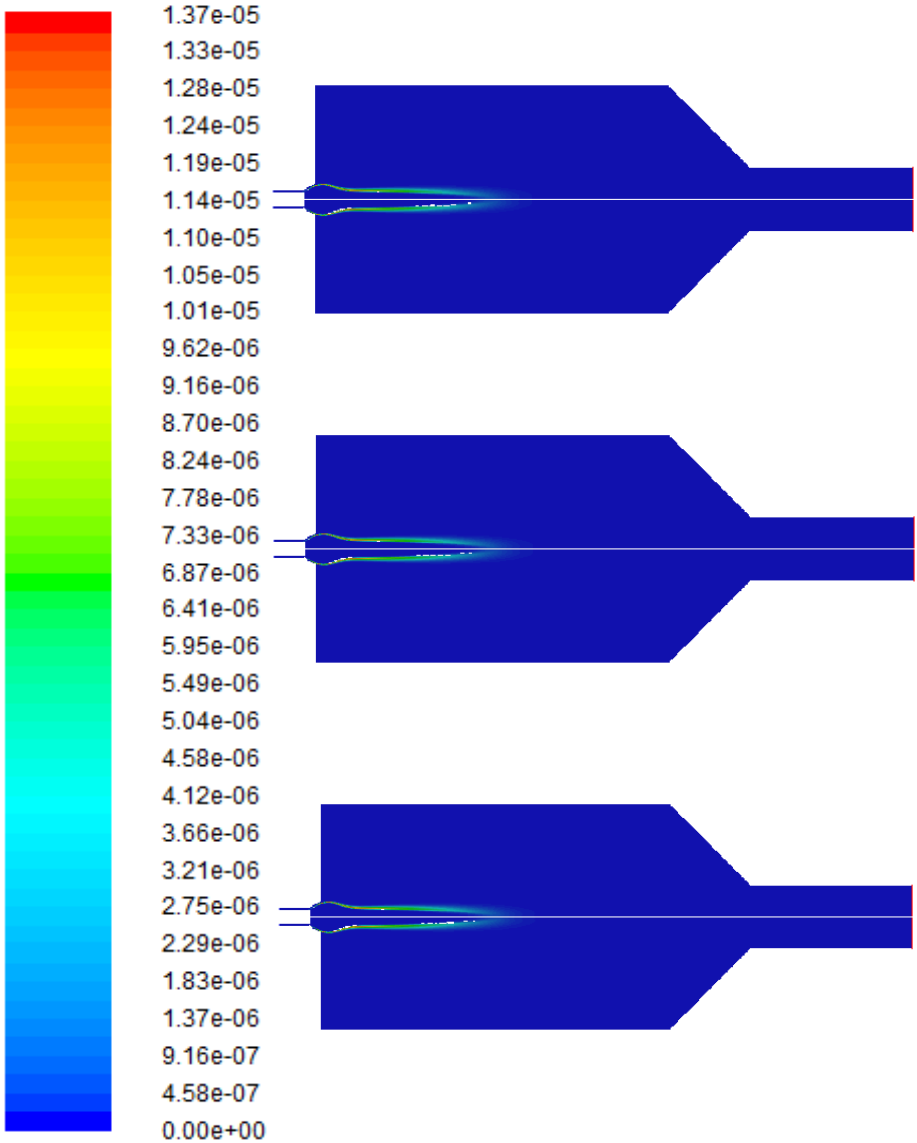


Figure 40: Biomethane prompt NO_x rate profiles. From up to down: 0%, 5% and 10% water in air.

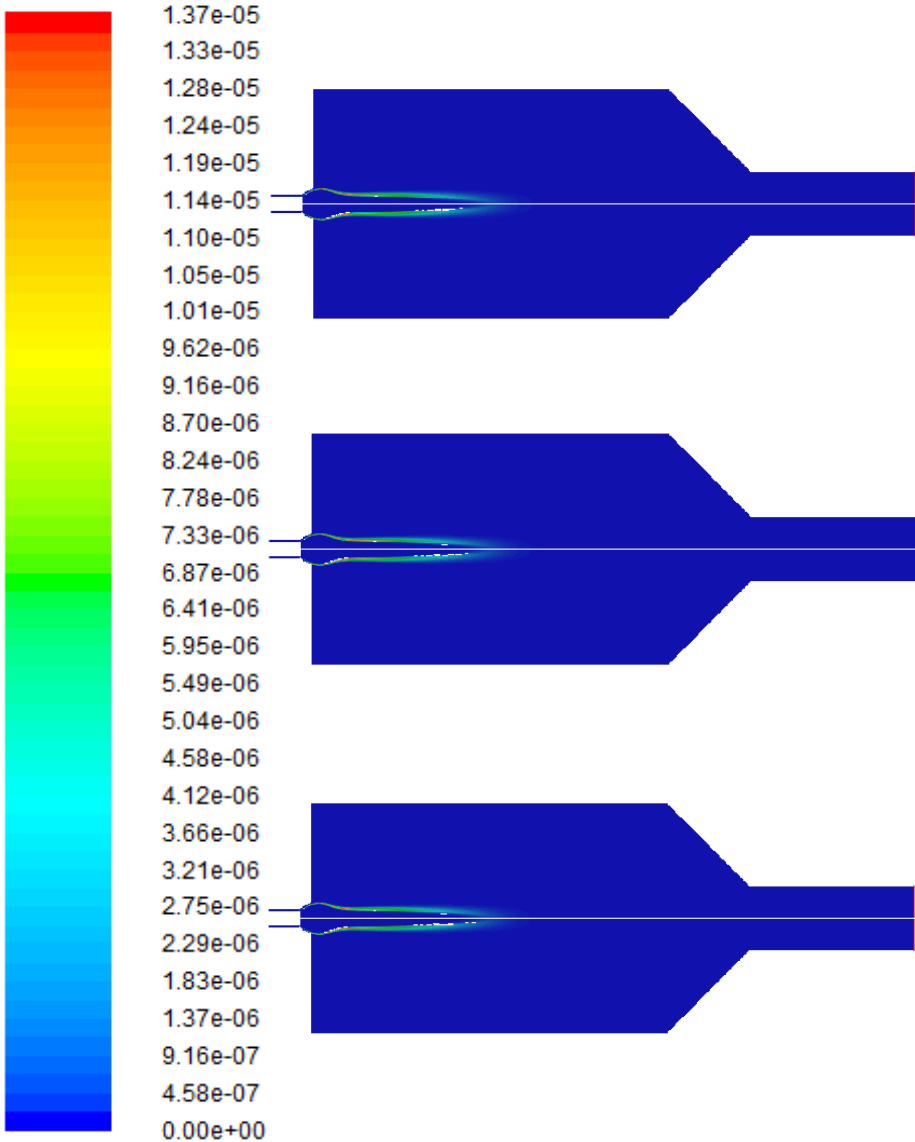


Figure 41: Biomethane prompt NO_x rate profiles. From up to down: 15%, 20% and 25% water in air.

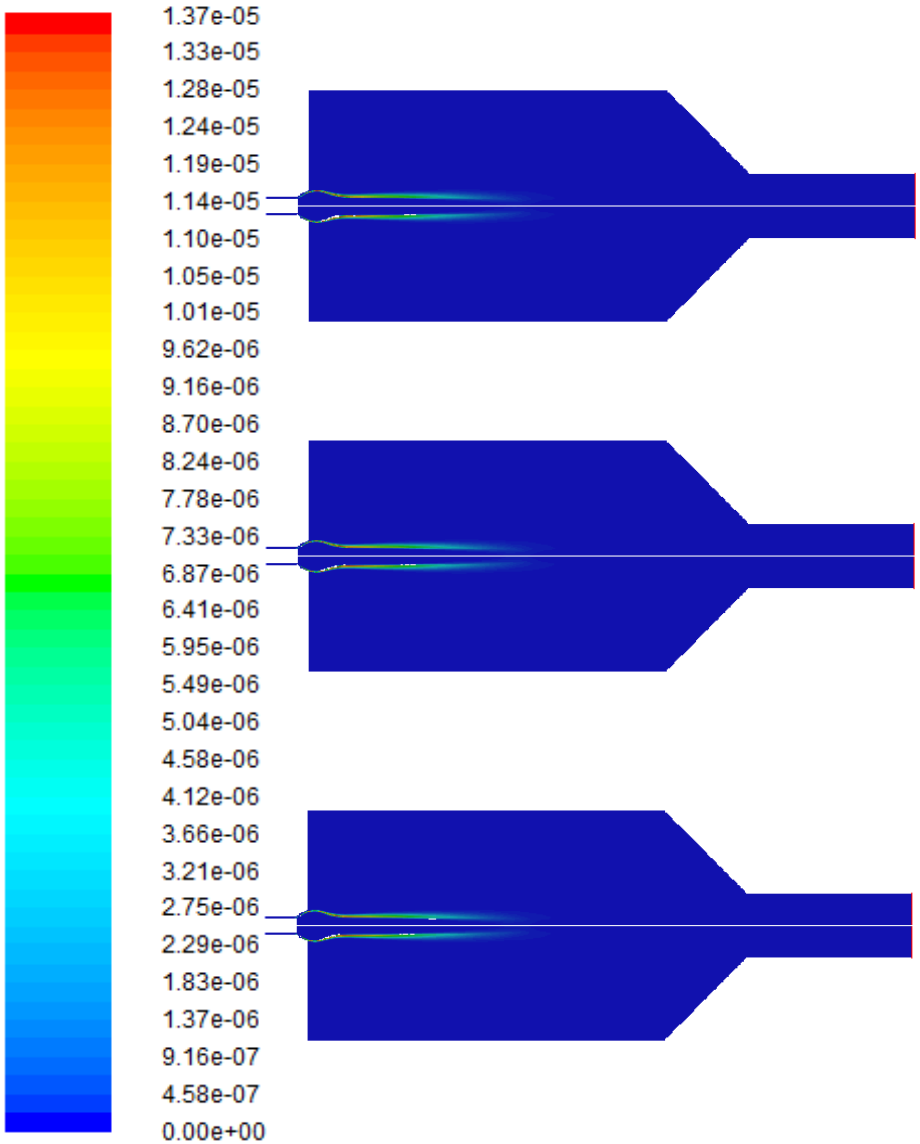


Figure 42: Methane prompt NO_x rate profiles. From up to down: 0%, 5% and 10% water in fuel.

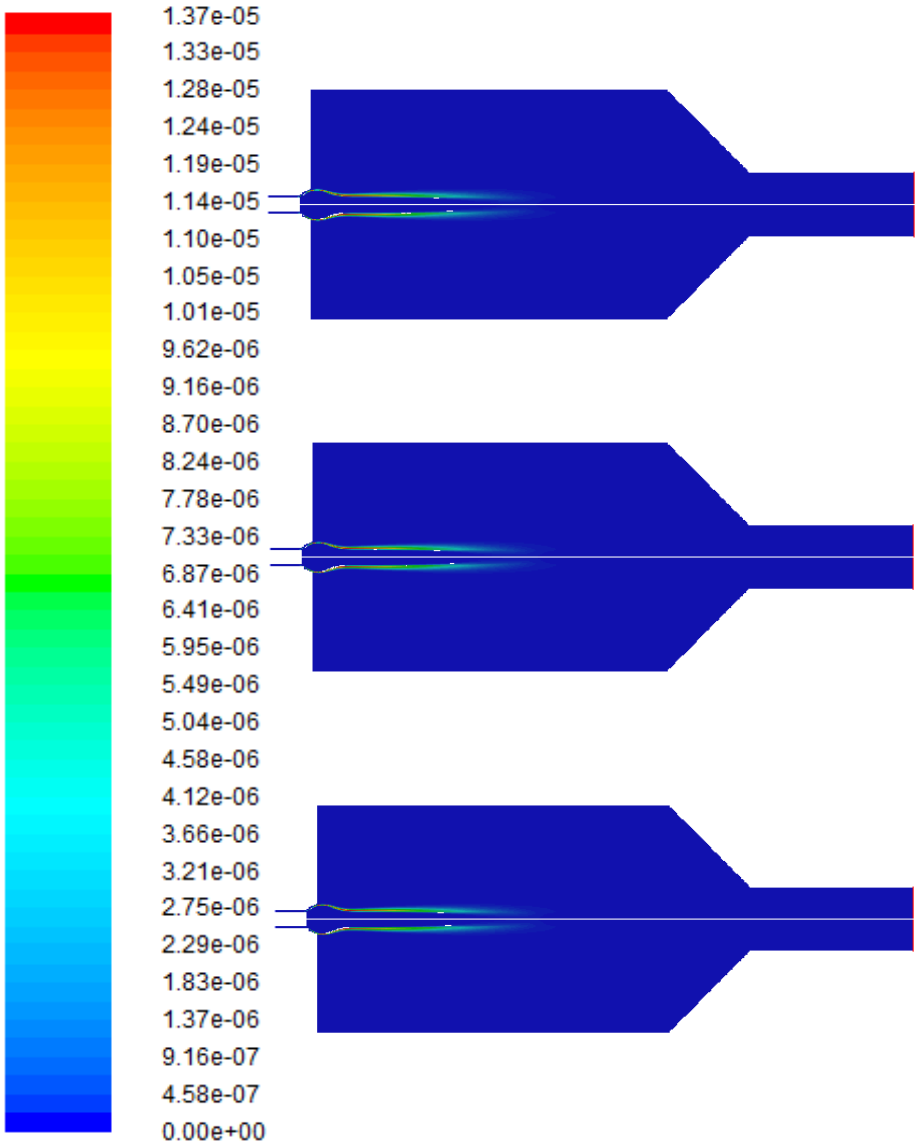


Figure 43: Methane prompt NO_x rate profiles. From up to down: 15%, 20% and 25% water in fuel.

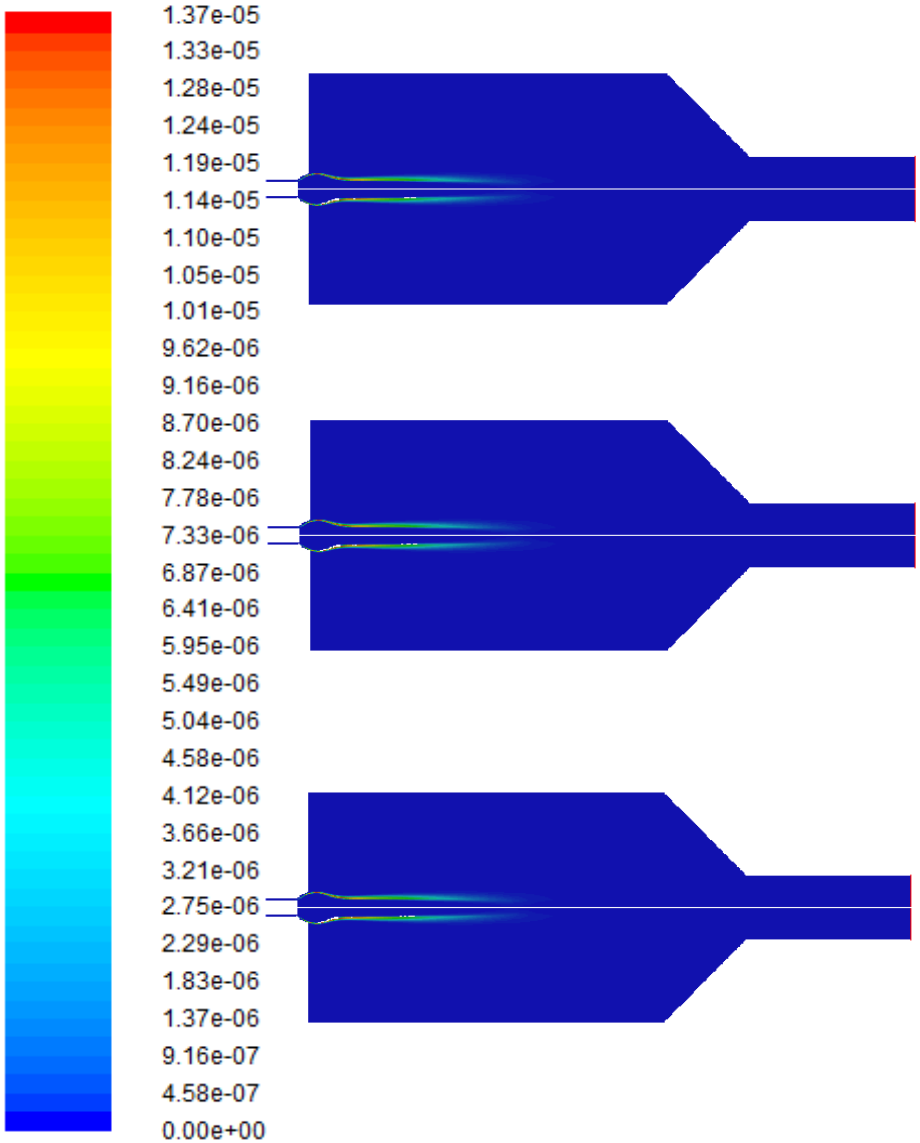


Figure 44: Methane prompt NO_x rate profiles. From up to down: 0%, 5% and 10% water in air.

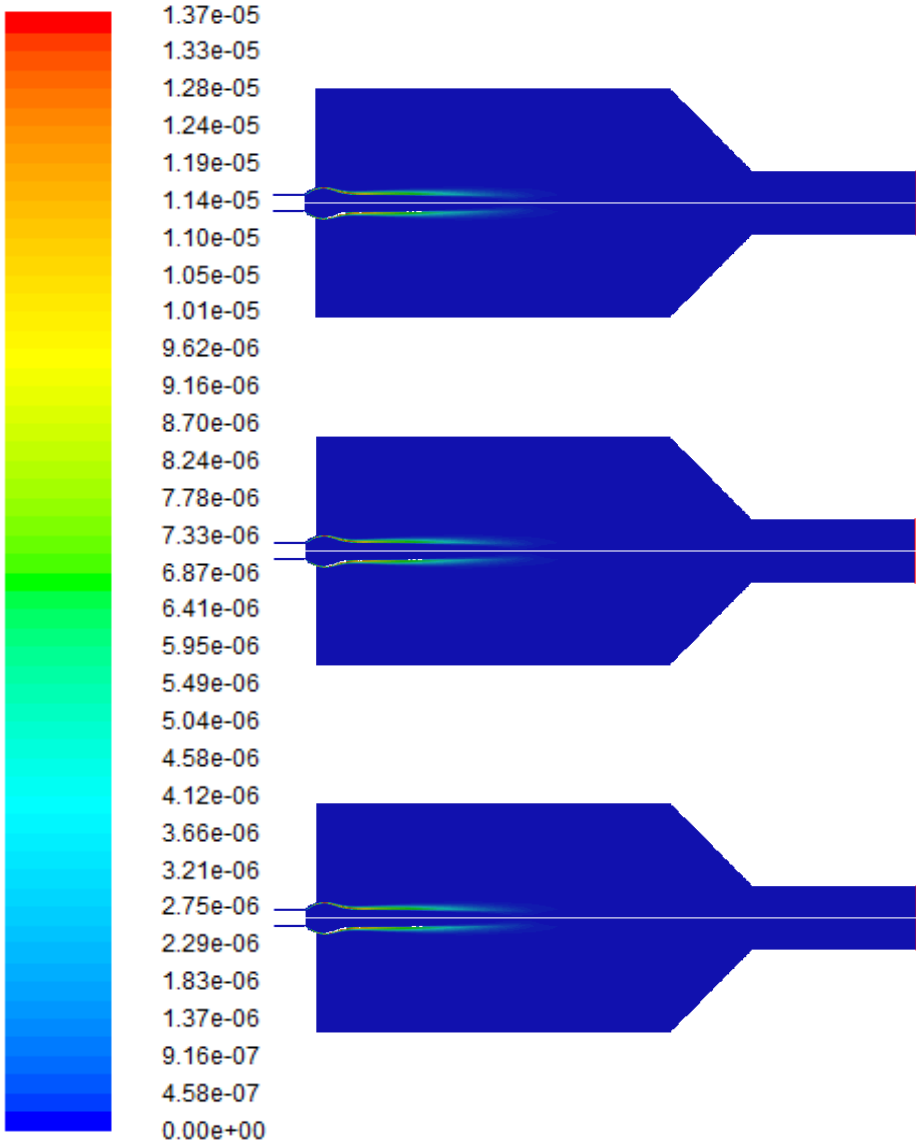


Figure 45: Methane prompt NO_x rate profiles. From up to down: 15%, 20% and 25% water in air.

